UNIVERSITÉ DU QUÉBEC À MONTRÉAL

CHANGEMENTS PALÉOCÉANOGRAPHIQUES DANS LA RÉGION DE DISKO BUGT, GROENLAND, AU COURS DE L'HOLOCÈNE

MÉMOIRE

PRÉSENTÉ

COMME EXIGENCE PARTIELLE

DE LA MAÎTRISE EN SCIENCES DE LA TERRE

PAR

MARIE-MICHÈLE OUELLET-BERNIER

SEPTEMBRE 2014

REMERCIEMENTS

Je tiens à remercier très sincèrement mes directeurs de recherche Anne de Vernal et Claude Hillaire-Marcel pour leur soutien, leur aide et les opportunités offertes sur le plan scientifique.

Je souhaite aussi remercier Maryse Henry, Audrey Limoges et Nicolas Van Nieuwenhove pour leur précieuse aide avec l'identification et l'interprétation des kystes de dinoflagellés. Je tiens aussi à remercier mes collègues de micropaléontologie pour leur appui et leur amitié. Je remercie aussi Sophie Retailleau pour son aide avec l'identification des foraminifères benthiques ainsi que Jean-François Hélie et Agnieszka Adamowicz pour leur aide au laboratoire d'isotopes stables.

Mes remerciements vont aussi à ma famille, et à mon amoureux Charles-Alexandre pour son appui à tout moment.

DÉDICACE

À mon petit Colin

AVANT-PROPOS

Ce mémoire est une contribution au projet Past4Future du 7^{e} Programme de la Commission européenne ainsi qu'une collaboration avec Matthias Moros du *Leibniz Institute for Baltic Sea Research*, Warnemuende, en Allemagne. Les échantillons étudiés ont déjà fait l'objet de nombreuses analyses notamment pour ce qui concerne les assemblages de foraminifères benthiques (Perner *et al.*, 2013 ; Perner *et al.*, 2011). Les datations au carbone 14 ont été fournies par Matthias Moros. Le présent mémoire contient des informations complémentaires à celles déjà disponibles. Les résultats obtenus ici sont originaux et apportent des éléments probants pour ce qui a trait aux changements des conditions océaniques le long des marges groenlandaises à l'Holocène. Le mémoire a été rédigé sous forme d'un article qui est soumis et accepté avec révisions mineures pour publication dans une revue thématique à comité de lecture, *The Holocene*. L'article a été rédigé en langue anglaise pour répondre aux exigences de la revue. La rédaction a été réalisée avec la collaboration de Madame Anne de Vernal et Messieurs Claude Hillaire-Marcel et Matthias Moros.

TABLE DES MATIÈRES

LISTE DES FIGURES

LISTE DES TABLEAUX

RÉSUMÉ

L'océanographie de la région de Disko Bugt est influencée par le glacier Jakobshavn Isbrae qui draine une partie de la calotte groenlandaise vers la mer. Les interactions entre les masses d'eau et ce dernier ont été documentées à partir d'une carotte de sédiment marin (MSM343300) prélevée sur le plateau continental à 518 m de profondeur, à 68°28,311'N et 54°00,118'W. D'une part, une analyse palynologique a été réalisée en portant une attention particulière aux kystes de dinoflagellés (dinokystes) qui permettent de caractériser les conditions océaniques de surface. La technique des analogues modernes a permis de reconstituer quantitativement les températures de surface, la salinité et le couvert de glace de mer. D'autre part, l'analyse isotopique de tests de foraminifères benthiques a permis de caractériser les propriétés de la masse d'eau découlant du Courant ouest groenlandais.

De ~10 000 à ~9250 ans calibrés (cal.) BP (*Before Present*), la composition isotopique ($\delta^{18}O$) des foraminifères benthiques indique une température basse et une salinité relativement élevée dans les eaux de fond. Vers 9250 ans cal. BP, une transition vers des eaux plus chaudes s'écoulant vers la baie de Baffin est enregistrée. Toutefois, les assemblages de dinokystes indiquent qu' en surface, les conditions sont restées rigoureuses avec un couvert de glace de mer dense et une productivité faible jusque vers 7300 ans cal. BP. À partir de ce moment, s'entame la période postglaciaire marquée par la diversification des espèces dans les assemblages de dinokystes jusqu'alors limités aux taxons hétérotrophes. La pénétration tardive des eaux atlantiques via le Courant ouest-groenlandais en surface serait en partie due aux apports de fonte glaciaire importantes de la calotte groenlandaise qui rendrait ainsi compte d'une couche dessalée en surface et d'une forte stratification dans les masses d'eau. Un optimum thermique avec des températures de surface ~10-12°C en été est finalement enregistré à partir de ~6000 ans cal. BP. En profondeur, on reconstitue une augmentation des températures d'environ 1°C. Dans les eaux de surface, l'optimum thermique est interrompu par deux épisodes de refroidissement, de ~4200 à 4000 et de ~1500 à 1000 ans cal. BP. Finalement, de ~1000 à ~800 ans cal. BP, la température de surface augmente jusqu'à atteindre ~10°C alors que la moyenne actuelle est de ~4,4°C (NODC, 2001). Il s'agit sans doute d'un intervalle correspondant à la période chaude médiévale.

Dans la série postglaciaire analysée, il est intéressant de noter l'opposition entre la température et la salinité. Lors d'épisodes chauds, la température augmente alors que

la salinité diminue résultant sans doute d'une augmentation des apports d'eaux de fonte en provenance des marges du Groenland et créant ainsi une stratification accrue des eaux de surface induisant un fort réchauffement estival.

MOTS-CLÉS : Dinokystes, foraminifères, Holocène, Courant ouest groenlandais, baie de Baffin, température de surface.

INTRODUCTION

L'Arctique est un milieu vulnérable vis-à-vis les changements du climat. Les effets d'une augmentation ou diminution de température y apparaissent de manière marquée notamment par l'augmentation ou la réduction du couvert de glace de mer, les avancées et les reculs de glaciers et la migration de la faune et de la flore (IPCC, 2012). Depuis la dernière glaciation, l'Arctique a subi des fluctuations climatiques, des réchauffements et refroidissements jusqu'à récemment attribuables à des facteurs naturels, tels que l'activité solaire et les paramètres orbitaux (e.g. Berger, 1988 ; Bond *et al.*, 2001). Or, actuellement, sur une courte période et de façon accélérée, nous assistons à la détérioration du pergélisol, à la diminution du couvert de glace de mer et à la fonte des glaciers et calottes glaciaires (Holland *et al.*, 2008 ; IPCC, 2012). De manière globale, la température estivale de l'air a augmenté de ~0,74°C entre 1905 et 2005; l'augmentation du niveau de la mer a été évaluée à 1,7 ± 0,5 mm/an entre 1901 et 2010 et de 3,2 ± 0,7 mm/an entre 1993 et 2010 (GIEC, 2013). L'Arctique est maintenant l'objet d'une attention particulière tant en lien avec les changements du climat et de l'environnement qu'avec l'impact sur les populations humaines et animales. Les perturbations climatiques actuelles sont souvent attribuées à des pressions anthropiques, mais il apparait important d'approfondir nos connaissances sur l'évolution naturelle du climat afin de mieux cerner les mécanismes en cause.

L'ouest du Groenland

Les marges de la calotte glaciaire groenlandaise qui atteignent les côtes et s'écoulent vers le plateau continental sont influencées par les fluctuations de température de l'océan. La récente augmentation de la température des eaux atlantiques entraine ainsi

une accélération du retrait glaciaire et une augmentation des eaux de fonte (Holland *et al.*, 2008 ; Rignot et Kanagaratnam, 2006). La fonte de la calotte groenlandaise rendrait compte d'une hausse du niveau marin de ~0,34 mm/an pour la période 1996-2005 (Rignot et Kanagaratnam, 2006).

Dans cette perspective, la région de Disko Bugt est particulièrement intéressante du fait qu'elle est située en aval d'un des glaciers des plus dynamiques de la calotte groenlandaise. Le Jakobshavn Isbrae draine près de 7% de la calotte groenlandaise (Roberts et Long, 2005) produisant une grande quantité d'icebergs (Weidick et Bennike, 2007). En 2003, la vélocité du retrait glaciaire du Jakobshavn Isbrae a atteint 12,6 km/an (Joughin, Abdalati et Fahnestock, 2004) entrainant des apports d'eaux de fonte et diluant les eaux de surface marine. D'un point de vue océanique, la région est baignée par le Courant ouest-groenlandais. Celui-ci se forme à la pointe sud du Groenland où le Courant Irminger composé d'apports d'eaux chaudes et salées de l'Atlantique nord et le Courant est-groenlandais composé d'apports froids et peu salés se rencontrent (Buch, 1982 ; Tang *et al.*, 2004). La baie de Disko est aussi marquée par une vitesse de sédimentation importante ce qui permet de produire des reconstitutions paléocéanographiques à haute résolution temporelle.

Dans ce mémoire, une attention spéciale est portée à la dynamique des échanges océan-glacier en caractérisant les conditions hydrographiques de la région de Disko Bugt. Afin de mesurer ceux-ci, une carotte de sédiment marin a été prélevée au large des côtes du Groenland. Les eaux de sub-surface y sont sous influence du Courant ouest-groenlandais, alors que les eaux de surface sont directement affectées par les décharges d'eaux de fonte des marges groenlandaises. À partir des indicateurs micropaléontologiques, il sera possible de dégager des signaux en provenance respectives des eaux de surface et des eaux atlantiques au cours de l'Holocène. L'analyse des dinokystes servira aux reconstitutions des conditions de surface incluant la température, la salinité, la glace de mer et la productivité dans le but

d'évaluer les apports d'eaux de fonte en provenance du Jakobshavn Isbrae et leurs effets sur l'environnement. Les analyses isotopiques ($\delta^{18}O$ et $\delta^{13}C$) à partir des tests de foraminifères benthiques apportent des informations sur la masse d'eau profonde et l'influence du Courant ouest-groenlandais. Combinés ces deux «proxys» permettront de retracer la pénétration du Courant ouest-groenlandais en profondeur et en surface.

CHAPITRE I

PALEOCEANOGRAPHIC CHANGES IN THE DISKO BUGT AREA, WEST GREENLAND, DURING THE HOLOCENE

Marie-Michèle Ouellet-Bernier[1,*], Anne de Vernal[1], Claude Hillaire-Marcel[1] and Matthias Moros[2]

[1]**Geotop, Université du Québec à Montréal, Canada**

[2]**Leibniz Institute for Baltic Sea Research Warnemuende, Germany**

*Corresponding author: Email: marie.michele.ob@hotmail.com

ABSTRACT

Micropaleontological analyses of a sediment core raised in Disko Bugt (West of Greenland) were undertaken in order to document paleoceanographical changes in the eastern Baffin Bay during the Holocene. The modern analogue technique (MAT) applied to dinocyst assemblages provided information on paleo-sea-surface conditions whereas isotopic analyses of benthic foraminifers aimed at documenting the "deep" water mass occupying the site. During the earlier interval recorded (~10 to ~7.3 cal. ka BP), important discharge of ice and meltwater from the Greenland ice sheet (GIS) margin, notably through the Jakobshavn Isbrae, resulted in harsh conditions with a dense sea-ice cover and low temperatures, productivity and foraminiferal abundances. Postglacial conditions settled at ~7.3 cal. ka BP, with a sharp rise in dinocyst abundance and species diversity, which led to an increase in reconstructed summer temperatures. We link this transition to the advection of West Greenland Current waters in the upper part of the water column after the reduction of meltwater inputs from GIS. Optimal temperature conditions reaching up to > 10°C were finally achieved in surface waters at ~6 cal. ka BP. Slight cooling pulses were then recorded at ~4.2-4 and ~1.5-1 cal. ka BP and the final optimum recorded in surface temperature from ~1 to 0.8 cal. ka BP is associated with the Medieval Warm Period. Throughout the postglacial interval, the data suggest an opposition between sea-surface temperatures and salinity, with warmer intervals being characterized by lower salinity waters, probably as a result as the higher freshwater discharge along the ice margin and notably the Jakobshavn Isbrae.

Keywords: dinocysts, foraminifers, Holocene, West Greenland, Baffin Bay, sea-surface temperature.

1.1 Introduction

Disko Bugt is an area of interest with regard to ocean-ice dynamics because it is located on the western margin of Greenland, where flows the Jakobshavn Isbrae, the largest and fastest ice stream of the Northern Hemisphere (Bindschadler, 1984). Disko Bugt is bathed by the West Greenland Current (WGC), which constists of a mixture of waters from the East Greenland Current (EGC) and Atlantic waters from the Irminger Current (IC). A warming trend of the WGC, accompanied by significant acceleration of glacier retreats and meltwater discharges has recently been recorded (Holland et al., 2008; Rignot and Kanagaratnam, 2006). The Jakobshavn Isbrae currently drains 7% of the Greenland Ice Sheet (GIS) (Roberts and Long, 2005) and produces a large amount of icebergs (Weidick and Bennike, 2007). In 2003, the velocity of the Jakobshavn Isbrae reached 12.6 $km.yr^{-1}$ (Joughin et al., 2004). Ongoing ice discharges from the GIS contribute significantly to the sea level rise, with values of 0.34 $mm.yr^{-1}$ from 1996 to 2005 (Rignot and Kanagaratnam, 2006).

In order to explore the relationship between the Jakobshavn Isbrae dynamics and the oceanographic conditions during the Holocene, we have analyzed a marine sediment core from Disko Bugt (core MSM343300; Figure 1). A first objective was to document long-term changes of the WGC, in particular that of the subsurface layer, which is mostly influenced by the northward flow of North Atlantic waters. A second objective was to reconstruct sea-surface temperature and salinity to assess the impact of meltwater discharge from Jakobshavn Isbrae on marine conditions at the mouth of Disko Bugt. To meet these objectives, we used organic-walled and calcareous microfossils as tracers of surface water masses properties. Palynological analyses were performed with special attention to dinoflagellate cysts, which permit the quantitative reconstruction of summer sea-surface temperature (SST), salinity (SSS), sea ice cover and primary productivity (e.g. de Vernal and Rochon, 2011). In addition, isotopic analyses ($\delta^{18}O$ and $\delta^{13}C$) of benthic foraminifer shells were made on two different species, *Islandiella norcrossi* and *Nonionellina labradorica* as a

means to document the properties of bottom waters, which correspond to the deeper part of the WGC, mostly its "warm" component from the North Atlantic.

1.2 Study area

Disko Bugt is a large marine embayment with water depths ranging mostly from 200 to 400 m and reaching up to 900 m in the Egedesminde Dyb trough (Long and Roberts, 2003; Roberts and Long, 2005; Ó Cofaigh et al., 2013; Perner et al., 2011; Hogan et al., 2012). The trough is associated with the Jakobshavn Isbrae ice stream route and GIS melting path during glacial times (Long and Roberts, 2003). In the Disko Bugt area, the WGC constitutes a combination of the IC formed of warm and saline Atlantic waters from the North Atlantic Current (NAC) and the EGC, which consists of polar and low salinity waters (Buch, 1982; Tang et al., 2004). The area is also characterized by buoyant low-salinity surface waters resulting from GIS meltwater supplies (Andersen, 1981). The WGC today occupies sub-surface waters below 200 m, where temperature and salinity are 2.5-3.5°C and 34.5-34.8 psu respectively (Andersen, 1981). The surface waters are usually colder as they are influenced by the polar water from the EGC in addition to the regional run-off and meltwater discharge. Data compiled from the National Oceanographic Data Center (NODC, 2001) indicate summer sea-surface temperature of 4.4 ± 1.24°C and salinity ranging between 32.9 and 33.4 at the study site. The modern sea ice cover averages 3.8 ± 1.3 months.yr^{-1} for the period 1953 to 2003 (National Snow and Ice data center, 2003).

1.3 Material and Methods

1.3.1 Sediment core and chronology

The study core MSM343300 (68°28,311'N, 54°00,118'W, Figure 1) was collected by gravity coring during the June 2007 *Maria S. Merian* expedition. It was retrieved from 519 m water depth (Harff et al., 2007), southwest of Disko Bugt in the direct flow path of the WGC.

The chronology was established from 25 accelerator mass spectrometry (AMS) ^{14}C dates in mollusc shells and benthic foraminifers (Table 1, Figure 2). The AMS radiocarbon dates were calibrated using the Marine09 (Reimer et al., 2009) calibration curve in CALIB 6.0.2 (Stuiver and Reimer, 1993). A total air-sea reservoir correction of 550 years was applied. It includes the usual correction of 410 years and a ΔR of 140 ± 35 years established from two measurements on modern *Astarte* collected at 60-70 m of water depth (McNeely et al., 2006). Such reservoir correction is consistent with the one applied by e.g. Lloyd et al. (2011) and Perner et al. (2011; 2013).

1.3.2 Age-Depth profile

The age vs depth profile was established based on interpolation (Figure 2). For the interval younger than 7500 cal. yr BP, the age to depth relationship is the same as the one reported by Perner et al. (2013). Based on the age model, sedimentation rates at the coring site ranged from 0.5 to 0.9 mm.yr^{-1} during the last 10 000 years: they were approximately 0.82 mm yr^{-1} between ~10 000 and ~7300 cal. yr BP, 0.5 mm.yr^{-1} between 7300 and 2500 cal. yr BP and 0.9 mm.yr^{-1} between 2500 and 800 cal. yr BP. In the lower part of the core, from 597 to 1113 cm, five AMS ^{14}C dates yielded similar ages of about 10 000 to 10 200 cal. years BP, which indicate extremely rapid sediment accumulation.

1.3.3 Microfossil analyses

Sub-sampling was done at 4-cm intervals throughout the core, which provide a time resolution of 50 to 80 years. The sediment samples were processed according to the protocol of de Vernal et al. (1996). A volume of 1 to 3.5 cm^3 of dry sediment was sieved on 106 µm and 10 µm mesh sieves. The fraction between 10 and 106 µm was used for palynological preparation and the fraction > 106 µm was kept for the hand-picking of foraminifers.

1.3.3.1 *Palynological analyses.* In order to concentrate the organic remains, carbonate and silicate particles were dissolved by repeated chemical treatment with HCl (10%) and warm HF (48%). A small drop of the final residue was mounted on a microscope slides with glycerine jelly. Before sieving and chemical treatments, *Lycopodium clavatum* spore tablets were added to estimate palynomorph concentration (Mertens et al., 2009; Matthews, 1969). Counting and identification were performed with an Orthoplan Leitz optical microscope at 400x magnification. All palynomorphs were counted (dinoflagellate cysts, pollen grains, spores, *Halodinium* and organic linings of foraminifer). A special attention was paid to dinoflagellate cysts (hereafter dinocysts). At least 300 dinocysts were counted per sample, which provide statistically reliable data (Mertens et al., 2009). The taxonomic nomenclature was based on Rochon et al. (1999) and Radi et al. (2013).

1.3.3.2 *Quantitative reconstructions of sea-surface conditions from dinocyst assemblages.* Reconstructions for sea-surface parameters were made based on the modern analogue technique (MAT), which relies on similarities between fossil and modern assemblages instead of calibrations between sea-surface parameters and assemblages (Guiot and de Vernal, 2007). Hence, MAT can be applied for simultaneous reconstruction of different parameters and appears appropriate in the case of non-linear relationship between assemblages and climate parameters. MAT was applied using dinocyst assemblages to reconstruct sea-surface temperature (SST) and salinity (SSS) in summer, in addition to sea ice cover extent and mean annual productivity. All these parameters play a determining role in the distribution of dinocyst assemblages as shown from multivariate analyses (e.g. Rochon et al., 1999; de Vernal et al., 2001, 2005, 2013; Radi and de Vernal, 2008). Here, we have used the updated Geotop dinocyst database that includes 66 taxa after taxonomic standardization and 1492 reference sites from the mid- to high latitudes of the Northern Hemisphere (de Vernal et al., 2013). We have followed the procedure as described by de Vernal et al. (2005). The relative occurrence of taxa was logarithmic

transformed in order to emphasize the weight of accompanying taxa as they have usually a more narrow range of ecological affinities than dominant taxa, which are often opportunistic and cosmopolitan (de Vernal et al., 2005). After the log transformation of the taxa occurrence, the five closest modern analogues were identified to estimate past sea-surface conditions. Reconstructions are given as the most probable value, which is the mean of the sea-surface parameter for the 5 best analogues, weighted inversely to the distance between the fossil and modern spectra. The minimum and maximum possible values according to the set of identified analogues are also reported. In order to assess the error of prediction of the reconstructions, validation tests are made after splitting of the database, with 1/6 of the data points taken randomly being used to verify the ability of the approach to reconstruct the sea-surface parameters. The errors of prediction at $\pm 1\sigma$ level were found to be ±1.6°C for summer SST, ±2.6 for SSS, ± 1.4 months.year^{-1} for the sea ice cover and ± 55 gC m^{-2} for productivity. It is noted that the SSS error of prediction is large because the database includes low salinity environments (down to 5 psu), where the variability of surface conditions is particularly large. When considering only the > 30 and > 33 salinity domains, the summer SSS errors of prediction are ±1.3 and ±0.8 psu, respectively.

In this study, a special attention was paid to the genus *Islandinium*, as the specie *cezare* appears to have an important weight in salinity reconstruction where dinocyst diversity is low (cf. Ouellet-Bernier, 2014).

1:3.3.3 *Foraminifer processing.* The >106 µm fraction was used for foraminifer analyses. We did not analyzed benthic foraminifer assemblages, as they were previously described by Perner et al. (2013). The two dominant calcareous taxa, *Islandiella norcrossi* (Cushman, 1933) and *Nonionellina labradorica* (Dawson, 1860) were selected for isotopic measurements. These two species have different ecological affinities. *I. norcrossi* is a shallow infaunal species common in Arctic environment

characterized by high and stable salinities, in addition to relatively warm subpolar waters conditions (Knudsen et al., 2012; Polyak et al., 2002; Hald and Steinsund, 1996). The foraminifer *N. labradorica* is a deeper infaunal species, which is associated with episodic fresh phytodetritus production (Knudsen et al., 2012; Polyak et al., 2002; Murray, 2006; Rytter et al., 2002; Steinsund, 1994).

In the study core, the foraminifer shells of *I. norcrossi* occur sporadically prior to ~6100 cal. yr BP and continuously afterward (above 341 cm). Shells of *N. labradorica* records sporadic occurrences at ~8200, ~6000, ~5500-5100, ~4000-2800 and ~1900-1200 cal. yr BP. Although, *N. labradorica* was the second most abundant specie after *I.norcrossi*, it occurred in low abundance. Hence, two size fraction were used: 150-250 μm and >250 μm to collect enough specimens for isotope analyses.

1.3.3.4 *Oxygen and carbon isotope analyses ($\delta^{18}O$, $\delta^{13}C$) in foraminifer shells.* Approximately 15 tests of *I. norcrossi* (150-250 μm) and 10 tests of *N. labradorica* (>250 μm) were roasted under vacuum at 250°C for one hour. Then, they were analyzed with a Micromass Isoprime™ isotope ratio mass spectrometer in dual inlet mode coupled with a MultiCard™ preparation system. Samples were heated to a constant temperature (90°C) for at least 30 minutes. CO_2 from foraminifer shells was extracted after dissolution with H_3PO_4 (102%). An internal reference carbonate material (UQ6) calibrated on the V-PDB scale was used to correct measurements. The overall analytical uncertainty (±1σ) is better than ±0.05‰ for both $\delta^{13}C$ and $\delta^{18}O$, as determined from replicate measurements of the home standard material.

1.4 Results

1.4.1 Palynological assemblages and pelagic fluxes

The palynological assemblages were largely dominated by dinocysts. Their concentration ranged between 2040 cysts g^{-1} and 171 500 cysts g^{-1} suggesting very high pelagic productivity at least during the middle and late Holocene (Figure 3).

Average fluxes of 3400 cysts $cm^{-2}.yr^{-1}$ were calculated in the interval spanning ~10 000 to ~7300 cal. yr BP (625-405 cm) while they ranged from ~2000 to ~20 000 cysts $cm^{-2}.yr^{-1}$ in the upper part of the sequence.

Pollen grains were present in low numbers (< 1400 grains g^{-1}). *Picea*, *Pinus* and *Betula* were the most common taxa. Low numbers of *monolete and trilete spores, including Lycopodium spp., were observed.* Concentrations of organic linings of foraminifers (cf. de Vernal et al., 1992) were relatively high, ranging between 550 and 234 000 linings g^{-1}, with maximum abundance during the middle and late Holocene. Concentrations of organic linings were significantly higher than those of calcareous shells of benthic foraminifers. Since the linings were observed in the 10-106 μm fraction while shells were counted in the >106 μm fraction, the higher lining abundances might either indicate some calcium carbonate dissolution in the sediment (cf. de Vernal et al., 1992) or a much higher abundance of small lining-bearing benthic foraminifers in the < 106 μm fraction and probably both. High concentrations of the acritarch *Halodinium* were recorded with up to 31 200 specimens g^{-1}. *Halodinium* has still unknown biological affinities, but it is generally associated with shallow marine and estuarine environment (e.g. Verhoeven et al., 2014), notably in cold arctic-subarctic settings marked by freshwater-meltwater inputs (de Vernal et al., 1989; Richerol et al., 2008).

1.4.2 Dinocyst assemblages

Dinocyst assemblages showed moderately high species diversity, with a maximum of 15 species, 9 being common to abundant (Table 2, Figure 3). The assemblages were dominated by *Islandinium minutum,* which was accompanied by the cyst of *Pentapharsodinium dalei*, *Brigantedinium* spp., *Operculodinium centrocarpum*, *Spiniferites elongatus*, *Selenopemphix quanta* and *Islandinium*? *cezare*. *Nematosphaeropsis labyrinthus* and *Spiniferites ramosus* occurred in very low number. The dinocyst assemblages permit to identify two main zones (Figure 3).

Zone I covers from ~10 000 to ~7300 cal. yr BP. The assemblage was composed almost exclusively of heterotrophic taxa, notably *Islandinium minutum*, which largely dominates, and *Brigantedinium* spp.. *I. minutum* occurs mostly in neritic environments, where it can thrive under a wide range of temperature and salinity conditions, but generally dominates in environments characterized by cold conditions and dense seasonal sea ice cover (Buck et al., 1998; Rochon et al., 1999; de Vernal et al., 2001, 2008, 2013). *I. minutum* has recently been shown to live under sea ice (Potvin et al., 2013). *Brigantedinium* spp. is a cosmopolitan taxon, which can be abundant in polar environments (Kunz-Pirrung, 2001; Rochon et al., 1999; Matthiessen et al., 2005).

Zone II covers from ~7300 to ~800 cal. yr BP and was defined from the increase of the *P. dalei* (Dale, 1996; Rochon et al., 1999), which reaches up to 40%, and the occurrence of other taxa such as *S. elongatus*, *S. ramosus*, *N. labyrinthus* and *S. quanta*. The taxa *S. elongatus* and *S. ramosus* are generally found in association with Atlantic waters (Rochon et al., 1999; Zonneveld et al., 2001; Marret and Scourse, 2003). *S. elongatus* prefers cool to temperate conditions (Rochon et al., 1999), whereas *S. ramosus* is more cosmopolitan and occurs in tropical to subpolar environments (e.g. Rochon et al., 1999; Zonneveld et al., 2001). *N. labyrinthus* develops in temperate to subpolar latitudes and prefers open oceanic environments (de Vernal et al., 2001; Kunz-Pirrung, 2001). *S. quanta* is cosmopolitan and occurs in temperate to subpolar environments (Rochon et al., 1999). It is abundant in upwelling zones and in areas of high nutrient concentration (Dale and Fjellså, 1994; Sangiorgi et al., 2002).

1.4.3 Reconstruction of sea-surface conditions

Close modern analogues of dinocyst assemblages were found for all samples and are located mostly in the Arctic Ocean and/or subpolar North Atlantic. The high concentration of dinocysts allowing statistically reliable counts (> 300 counted

specimens/sample) and the high degree of similarity between the fossil assemblages and their modern analogues permit to be as confident as possible with the reconstruction from MAT

In zone I, the reconstructions indicated cold conditions with summer SST averaging 1.5°C, almost 9 months.yr^{-1} of sea ice cover and very low primary productivity (100 gC m^{-2}.yr^{-1}). SSS was relatively high (~31.5 psu) during the interval.

In Zone II, which is characterized by an increase in species diversity, the MAT-based reconstructions showed a gradual warming in surface waters. From ~7300 to ~7000 cal. yr BP, SST increased rapidly up to ~7°C, while salinities decreased to ~30.5 psu and sea ice cover was reduced to 5-6 months.yr^{-1}. Optimal conditions finally established at ~6000 cal. yr BP, with average summer SSTs of about 9-10°C. During this interval, SSS were low, around 28-30 psu, sea ice cover was restricted to the winter season, and productivity slowly increased up to ~ 400 gC m^{-2}.yr^{-1}. Cooling pulses were recorded at ~4000-4200 and ~1500-1000 cal. yr BP. They correspond to increase in salinity (up to ~32 psu), which we interpret here as the result of reduced meltwater discharge.

1.4.2 Isotopic composition of benthic foraminifer shells

The isotopic analyzes allowed the establishment of a discontinuous record with large gaps before ~6300 cal. yr BP due to the rarity of specimens (Figure 5). After ~6300 cal. yr BP, the record is more continuous.

The taxon *I. norcrossi* usually records $\delta^{18}O$ and $\delta^{13}C$ values close to equilibrium with bottom sea-water, which makes it a useful paleoceanographic tracer (Ishimura et al., 2012). Zone I was characterized by high $\delta^{18}O$ values (~4.0‰) from ~10 000 to ~9250 cal. yr BP, which reflect cold water conditions with a near standard mean ocean water salinity. It however depicted variable $\delta^{13}C$ values, ranging between

-1.91 and -0.53‰, with particularly low values (-4.72‰) around 8200 cal. yr BP. This light ^{13}C excursion appeared significant since it was recorded in both taxa analyzed, *I. norcrossi* and *N. labradorica*. Zone II was marked by $\delta^{18}O$ values ranging 3.56 to 3.1‰ from ~6100 to ~960 cal. yr BP and by $\delta^{13}C$ ranging between -0.69 and -0.08‰.

The sporadic occurrences of *N. labradorica* could be related to episodes of high sea-surface productivity (e.g. Jennings et al., 2004; Mudie et al., 1984; Polyak and Solheim, 1994; Wollenburg and Mackensen, 1998; Rytter et al., 2002; Polyak et al., 2002; Hald and Steinsund, 1992; Mackensen et al., 2001). *N. labradorica* recorded $\delta^{18}O$ values ranging from 3 to 3.57‰, which was very close to those observed in *I. norcrossi*. With respect to $\delta^{13}C$, *N. labradorica* usually yielded higher values than *I. norcrossi,* which may be related to the direct influence of high seasonal productivity of fresh phytodetritus (Knudsen et al., 2012; Polyak et al., 2002; Murray, 2006; Rytter et al., 2002). As mentioned above, in Zone I, the $\delta^{13}C$ of *N. labradorica* was characterized by particularly low values at ~8200 cal. yr BP (-6.41 to -6.03‰), consistent with the isotopic excursion recorded by *I. norcrossi*. In Zone II, *N. labradorica* recorded larger variations than *I. norcrossi,* with values ranging from -2.93 to -0.74‰.

1.5 Discussion

1.5.1 The deglaciation phase from ~10 000-~7300 cal. yr BP

Important changes occurred in surface and bottom waters in the study area during the deglaciation and the Holocene. In the Disko Bugt area, the glacial retreat began after 13 800 yr BP (Ó Cofaigh et al., 2013). From the adjacent core MSM343340 (Figure 1), it was suggested that a fast ice retreat started at about 12 050 cal. yr BP, with a retreat rate of ~22-275 m a^{-1} (Ó Cofaigh et al., 2013). By 10 900 cal. yr BP, the ice margin had retreated at the mouth of Disko Bugt, where glacier ablation resulted in high terrigenous input from 10 140 to 8490 cal. yr BP (Jennings et al., 2014). The

extremely high sedimentation rates recorded in our core at about 10 000 cal. yr BP also suggesting a rapid sediment accumulation, which might be related with glaciomarine processes (Figure 2). According to Weidick and Bennike (2007), the deglaciation of Disko Bugt occurred rapidly during the early Holocene (~10 500 to ~10 000 yr BP). Long and Roberts (2003) also suggested that the Jakobshavns Isbrae recorded a rapid retreat after ~10 300 cal. yr BP with a velocity of about 4.8 $km.yr^{-1}$, approching the modern values of 6-7 $km.yr^{-1}$. Atmospheric temperature significantly increased from ~10 000 to ~8000 yr BP as indicated from the NGRIP ice core data (Vinther et al., 2006). Whereas the GIS margin was retreating, surface waters were characterized by a dense sea ice cover (> 9 $months.yr^{-1}$), low summer temperatures (0-3°C) and a low productivity (~100 $gC\ m^{-2}.yr^{-1}$), which is consistent with glaciomarine conditions. This is also compatible with the dominance of *Islandinium minutum* that can lives under pack ice (Potvin et al., 2013; Rochon et al., 1999). Moreover, high $\delta^{18}O$ values (~4‰) in benthic foraminifers indicate low temperatures and a relatively high salinity in bottom waters.

Glaciomarine conditions were documented to have prevailed until 7800 cal. yr BP based on tephra shards analyses and the occurrence of the agglutinated benthic foraminifer *Spiroplectammina biformis* (Jennings et al., 2014), which was associated with glacial meltwater (Schafer and Cole, 1986; Jennings and Helgadottir, 1994). Hence low surface salinity and stratification of the upper water column may have resulted from the occurrence of low salinity-cold surface waters, overlying warmer and more saline bottom waters linked to Atlantic water inputs. Glacier runoff probably slowed down as the glacier became land-based around 7700-7500 cal. yr BP (Young et al., 2011; Seidenkrantz et al., 2013). Widespread mollusc colonization and organic accumulation in coastal lakes began some 7500 years ago, after the retreat of the Jakobshavn Isbrae and/or GIS margin (Donner and Jungner, 1975; Briner et al., 2010; Fredskild, 2000). The postglacial warming along the southwest Greenland coastline was possibly delayed because of meltwater runoff along the Greenland

margins, as documented from diatoms in the Ameralik fjord where the WGC reached the surface only by ~7800 cal. yr BP (Ren et al., 2009; Seidenkrantz et al., 2013) as well as from many coastal lake pollen records (cf. Fréchette and de Vernal, 2009) (cf. Figure 6).

The light ^{13}C-excursion recorded by both benthic foraminifer species at ~8200 cal. yr BP deserves some attention. Based on the micropaleontological data presented here, neither surface conditions, nor benthic production or bottom water properties have changed significantly during the interval spanning from ~8200 to ~7000 cal. yr BP. We are thus tempted to link this excursion to a methane seepage event on the seafloor (Kaneko et al., 2010). Further geochemical analyses are underway to document this hypothesis.

1.5.2 First WGC influence ~7300 cal. yr BP

In surface waters of the Disko Bugt, the northward penetration of the WGC likely occurred at about 7300 cal. yr BP as shown by the dinocyst-based reconstruction of SSTs and sea ice cover. This transition was marked by an increase in dinocyst species diversity, with the significant occurrence of cysts of *Pentapharsodinium dalei*, *Operculodinium centrocarpum* and *Spiniferites ramosus*, in addition to *Selenopemphix quanta*. From ~7300 to ~6000 cal. yr BP, large amplitude warming of surface waters was recorded. The change in dinocyst assemblages led to reconstruct SSTs increase from 3°C to 10°C in summer, which was accompanied by a decrease in sea ice cover from > 8 to < 3 months.yr^{-1}. This change was also marked by an increase of annual productivity, which reached up to 350 gC $m^{-2}.yr^{-1}$. The transition from ~7300 to ~6200 cal. yr BP is also recorded in bottom waters as shown by the synchronous increase of benthic foraminifer species associated with Atlantic waters, such was *Islandiella norcrossi* and *Cassidulina reniforme* (Fig.6 ; Perner et al., 2013).

It is notable that the SST increase at ~7300 cal. yr BP was accompanied with a salinity decrease in surface waters, which suggests that warmer condition may have

led to accelerated glacier melting, resulting in enhanced freshwater discharges from the Jakobshavn Isbrae and/or the Greenland margins. Therefore, our data support the hypothesis of a delayed influence of WGC in the surface waters as compared to seafloor conditions, due to high meltwater supplies (Lloyd et al., 2005).

1.5.3 Mid-Holocene Optimal conditions from ~6000 cal. yr BP

Optimal conditions were established in surface waters from ~6000 cal. yr BP. The thermal optimum was locally characterized by sea ice cover restricted to the winter season (~3 months.yr^{-1}), high primary productivity (up to 300-400 gC m^{-2}.yr^{-1}), and summer SST reaching up to 10-12°C. The general salinity decrease to about 29 psu was possibly related with meltwater discharge from the ice margin when Jakobshavn Isbrae recorded its maximal retreat, which occurred by ~4000 cal. yr BP (Weidick et al., 1990; Weidick, 1992). Many paleoclimate studies of the southwest and western Greenland are consistent with the reconstructions of sea-surface conditions presented herein. Most of them suggest that optimum conditions were attained relatively late, from ~6000 to ~3500-3000 cal. yr BP (cf. Figure 6). In particular, Perner et al. (2013) have described an episode of high phytodetritus supply, coherent with the high surface primary productivity we reconstructed from our dinocyst assemblages. Moreover, St□Onge and St□Onge (2014) documented the ice margin retreat to the present position from 7000 to 6000 cal. yr BP based on magnetic susceptibility and density.

The dinocyst-based reconstruction shows cooling pulses at ~4200-4000 (down to 6°C) and ~1500-1000 cal. yr BP (down to 3-4°C). They could be associated with the Neoglacial cooling phase (e.g. Kelly, 1980; Dahl-Jensen, 1998; Kaufman, 2004; Miller et al., 2005). Hence, these cooling pulses seem to represent a consistent feature on regional scale. Diatom data from Disko Bugt also show a temperature decrease between ~4000 and ~3800 cal. yr BP (Moros et al., 2006). Similarly, in Ameralik Fjord, an episode of extensive sea ice cover and colder surface water was observed

from ~4400 to ~3600 cal. yr BP (Ren et al., 2009). The Neoglacial cooling period was recorded from ~3500 to ~2000-1800 yr BP in many regional reconstructions of climate changes (Andresen et al., 2010; Krawczyk et al., 2010; Lloyd et al., 2007; Perner et al., 2011, 2013) (Figure 6) correlated with a Jakobshavn Isbrae glacier readvance (St□Onge and St□Onge, 2014). Moreover, the second cooling phase we reconstruct at ~1500 cal. yr BP was also reported from microfossil data in the Disko Bugt area as the so-called Dark ages period. Krawczyk et al. (2010) and Seidenkrantz et al. (2008) reconstructed a cooling period from ~1500 to ~1300 cal. yr BP respectively based on diatom and dinocyst data. Seidenkrantz et al. (2007) suggested a cooling period from ~1600 to ~1200 based on benthic foraminifers analyses. Jensen et al. (2004) and Ribeiro et al. (2012) documented a cooling event from ~1450 to ~1250 yr BP (cal. AD 500 to 750) based on diatom and dinocyst data (Figure 6).

In addition to SST changes, the dinocyst data permitted to reconstruct surface salinity changes, which ranged from 29 to 32 psu during the interval. A striking feature is the almost systematic opposite trend of surface-water salinity and summer temperature: warm episodes correspond to low salinity conditions, and vice-versa, the coldest phase being marked by the highest salinity. The salinity vs temperature variations in the study core tend to support the hypothesis of accelerated Jakobshavn Isbrae melting and freshwater discharges under warm conditions in relation to the strength and/or the temperature of the WGC.

In bottom sediments, benthic foraminifers became abundant enough around 6000 cal. yr BP to establish a continuous isotopic record. The $\delta^{18}O$-values in *Islandiella norcrossi* slightly decreased from ~6000 to ~5000 cal. yr BP (from ~3.45 to 3.2‰), which might correspond to a temperature rise (≤1°C) of the bottom waters. This is consistent with the increase of *I. norcrossi* relative to Arctic species such as *Elphidium excavatum* and *Cassidulina arctica*, which together suggest a stronger Atlantic component in the WGC or reduced meltwater supplies through the EGC

(Lloyd, 2006a; Perner et al., 2013). Overall benthic foraminifer assemblages also showed a thermal maximum from ~6000 to ~5000 cal. yr BP, followed by a gradual cooling until ~3900 cal. yr BP (Lloyd et al., 2007; McCarthy, 2011; Perner et al., 2011, 2013).

$\delta^{18}O$-values in *I. norcrossi* slightly increased (up to ~3.32‰) from ~2100 to ~1100 cal. yr BP, thus suggesting a temperature decrease of the bottom waters matching that reconstructed at the sea-surface. The corresponding change in benthic foraminifer assemblages might be associated with an enhanced influence of the EGC (Perner et al., 2011, 2013; Jennings et al., 2011) relative to a decrease influence of the IC (Lloyd et al., 2007).

Finally, one should highlight the fact that productivity variations reconstructed from dinocysts are consistent with the occurrence of the phytodetritus feeder *Nonionellina labradorica* from ~6000 to ~5100 and ~4000 to ~2800 cal. yr BP (Jennings et al., 2004; McCarthy, 2011; Lloyd, 2006b).

1.5.4 Medieval warming (~1000-800 cal. yr BP)

From ~1000 to ~800 cal. yr BP, summer SSTs increased to about 10°C, which is much higher than the present day summer SST of ~4.4°C±1.24°C at the coring site. In the dinocyst assemblage, *I. minutum* percentages decreased whereas the *S. elongatus* percentages increase. We suggested that this event correspond to a warming of the WGC. Benthic foraminiferal analyses also led to suggest enhanced contribution of IC to the WGC from ~1400 to ~900 cal. yr BP (Perner et al., 2013). This event can be associated with a regional signature of the Medieval warm period as described, for example, by Dahl-Jensen (1998) from Greenland ice cores and by many others paleoceanographical proxies of the Disko Bugt and western Greenland areas (Andresen et al., 2010; Krawczyk et al., 2010; Lloyd et al., 2007; Perner et al., 2011; Ribeiro et al., 2012; Seidenkrantz et al., 2007) (Figure 6). Correlation with

records from Southern and Eastern Greenland (Jensen et al., 2004; Lassen et al., 2004; Kaplan, 2002; Anderson and Leng, 2004) and with Icelandic shelf (Eiríksson et al., 2000; Jiang et al., 2002) records might also be proposed.

1.6 Conclusion

We have attempted here to reconstruct paleoceanographical changes along the West Greenland margin during the Holocene from a multi-proxy approach with a better than centennial time resolution for some proxies. Dinocyst-based reconstructions provided information on sea-surface conditions and permitted to distinguish both temperature and salinity signals as a complex response to the northward flow of the WGC and freshwater discharge from the GIS. Data indicate glaciomarine conditions until ~10 000 cal. yr BP while the earliest evidence of some Atlantic influence through the WGC appeared in deep water, when the benthic foraminifer *Islandiella norcrossi* was first recorded in the core. The WGC influence was recorded much later in surface waters, which were characterized locally by cold conditions with a dense ice cover until ~7300 cal. yr BP, likely because of important discharge of ice and meltwater from the GIS. After a gradual transition marked by an increasing influence of Atlantic waters, optimal conditions finally settled at ~6000 cal. yr BP. Some cooling pulses were recorded later on, at ~4200-4000 and ~1500-1000 cal. yr BP, alternating with warm phases at ~6000-4200, ~4000-1500 and ~1000-800 cal. yr BP. Throughout the postglacial, there is an opposition between SSTs and surface salinities, with warmer intervals being characterized by more diluted surface water. We thus associate the warming linked to increasing influence of Atlantic waters through the WGC, to phases of enhanced melt, thus resulting in higher freshwater discharge from Greenland ice margins and notably from the Jakobshavn Isbrae. The Holocene paleoceanographical record of Disko Bugt presented herein tends to demonstrate close linkage between the ocean and ice dynamics.

1.7 Acknowledgments

This study is a contribution to the project Past4Future of the 7th Framework Program. We are grateful to Maryse Henry, Audrey Limoges and Nicolas Van Nieuwenhove for their precious help with dinocyst identification and interpretation. We also thank the Geotop Stable isotopes laboratory.

1.8 Funding

The authors thank the *Ministère du Développement Économique, Innovation et Exportation* (MDEIE) and *Fonds Québécois de Recherche sur la Nature et les Technologies* (FQRNT) and the Natural Sciences and Engineering Research Council of Canada (NSERC).

1.9 References

Andersen O. (1981) The annual cycle of temperature, salinity, currents and water masses in the Disko Bug and adjacent waters, West Greenland. *Meddelelserom Gronland, Bioscience* 5.

Anderson NJ and Leng MJ. (2004) Increased aridity during the early Holocene in West Greenland inferred from stable isotopes in laminated-lake sediments. *Quaternary Science Reviews* 23: 841-849.

Andresen CS, McCarthy DJ, Valdemar Dylmer C, et al. (2010) Interaction between subsurface ocean waters and calving of the Jakobshavn Isbrae during the late Holocene. *The Holocene* 21: 211-224.

Bindschadler RA. (1984) Jakobshavns Glacier drainage basin: A balance assessment. *Journal of Geophysical Research* 89: 2066.

Briner JP, Stewart HAM, Young NE, et al. (2010) Using proglacial-threshold lakes to constrain fluctuations of the Jakobshavn Isbræ ice margin, western Greenland, during the Holocene. *Quaternary Science Reviews* 29: 3861-3874.

Buch E. (1982) Review of oceanographic conditions in Sub area 0 and 1 during the 1970–79 decade. *NAFO Sci. Coun. Studies* 5: 43-50.

Buck KR, Nielsen TG, Hansen BW, et al. (1998) Infiltration phyto- and protozooplankton assemblages in the annual sea ice of Disko Island, West Greenland, spring 1996. *Polar Biology* 20: 377-381.

Dahl-Jensen D. (1998) Past Temperatures Directly from the Greenland Ice Sheet. *Science* 282: 268-271.

Dale B. (1996) Dinoflagellate cyst ecology: modeling and geological applications. *Palynology: principles and applications* 3: 1249-1275.

Dale B and Fjellså A. (1994) Dinoflagellate cysts as paleoproductivity indicators: state of the art, potential, and limits. *Carbon cycling in the glacial ocean: Constraints on the ocean's role in global change.* Springer, 521-537.

de Vernal A, Bilodeau G, Hillaire-Marcel C, et al. (1992) Quantitative assessment of carbonate dissolution in marine sediments from foraminifer linings vs. shell ratios: Davis Strait, northwest North Atlantic. *Geology* 20: 527.

de Vernal A, Eynaud F, Henry M, et al. (2005) Reconstruction of sea-surface conditions at middle to high latitudes of the Northern Hemisphere during the Last Glacial Maximum (LGM) based on dinoflagellate cyst assemblages. *Quaternary Science Reviews* 24: 897-924.

de Vernal A, Goyette C and Rodrigues CG. (1989) Contribution palynostratigraphique (dinokystes, pollen et spores) à la connaissance de la mer de Champlain: coupe de Saint-Césaire, Québec. *Canadian Journal of Earth Sciences* 26: 2450-2464.

de Vernal A, Henry M and Bilodeau G. (1996) Techniques de préparation et d'analyses en micropaléontologie. *Les cahiers du GEOTOP* 3.

de Vernal A, Henry M, Matthiessen J, et al. (2001) Dinoflagellate cyst assemblages as tracers of sea-surface conditions in the northern North Atlantic, Arctic and sub-Arctic seas: the new ?n = 677? data base and its application for quantitative palaeoceanographic reconstruction. *Journal of Quaternary Science* 16: 681-698.

de Vernal A, Hillaire-Marcel C, Rochon A, et al. (2013) Dinocyst-based reconstructions of sea ice cover concentration during the Holocene in the Arctic Ocean, the northern North Atlantic Ocean and its adjacent seas. *Quaternary Science Reviews* 79: 111-121.

de Vernal A, Hillaire□Marcel C, Solignac S, et al. (2008) Reconstructing sea ice conditions in the Arctic and sub□Arctic prior to human observations. *Arctic*

Sea ice Decline: Observations, Projections, Mechanisms, and Implications: 27-45.

de Vernal A and Rochon A. (2011) Dinocysts as tracers of sea-surface conditions and sea-ice cover in polar and subpolar environments. *IOP Conference Series: Earth and Environmental Science* 14: 012007.

Donner J and Jungner Hö. (1975) Radiocarbon dating of shells from marine Holocene deposits in the Disko Bugt area, West Greenland. *Boreas* 4: 25-45.

Eiríksson J, Knudsen KL, Haflidason H, et al. (2000) Late-glacial and Holocene palaeoceanography of the North Icelandic shelf. *Journal of Quaternary Science* 15: 23-42.

Fréchette B and de Vernal A. (2009) Relationship between Holocene climate variations over southern Greenland and eastern Baffin Island and synoptic circulation pattern. *Climate of the Past* 5.

Fredskild B. (2000) The Holocene vegetational changes on Qeqertarsuatsiaq, a West Greenland island. *Geografisk Tidsskrift-Danish Journal of Geography* 100: 7-14.

Guiot J and de Vernal A. (2007) Chapter Thirteen Transfer Functions: Methods for Quantitative Paleoceanography Based on Microfossils. 1: 523-563.

Hald M and Steinsund P. (1996) Benthic foraminifera and carbonate dissolution in the surface sediments of the Barents and Kara Seas. *Surface-sediment composition and sedimentary processes in the central Arctic Ocean and along the Eurasian Continental Margin. Berichte zur Polarforschung* 212: 285-307.

Hald M and Steinsund PI. (1992) Distribution of surface sediment benthic foraminifera in the southwestern Barents Sea. *The Journal of Foraminiferal Research* 22: 347-362.

Harff J, Dietrich R, Endler R, et al. (2007) Deglaciation History, Coastal Development, and Environmental Change during the Holocene in Western Greenland.

Hogan K, Dowdeswell J and Ó Cofaigh C. (2012) Glacimarine sedimentary processes and depositional environments in an embayment fed by West Greenland ice streams. *Marine Geology* 311: 1-16.

Holland DM, Thomas RH, de Young B, et al. (2008) Acceleration of Jakobshavn Isbræ triggered by warm subsurface ocean waters. *Nature Geoscience* 1: 659-664.

Ishimura T, Tsunogai U, Hasegawa S, et al. (2012) Variation in stable carbon and oxygen isotopes of individual benthic foraminifera: tracers for quantifying the vital effect. *Biogeosciences Discussions* 9: 6191-6218.

Jennings A, Andrews J and Wilson L. (2011) Holocene environmental evolution of the SE Greenland Shelf North and South of the Denmark Strait: Irminger and East Greenland current interactions. *Quaternary Science Reviews* 30: 980-998.

Jennings AE and Helgadottir G. (1994) Foraminiferal assemblages from the fjords and shelf of eastern Greenland. *The Journal of Foraminiferal Research* 24: 123-144.

Jennings AE, Walton ME, Ó Cofaigh C, et al. (2014) Paleoenvironments during Younger Dryas-Early Holocene retreat of the Greenland Ice Sheet from outer Disko Trough, central west Greenland. *Journal of Quaternary Science* 29: 27-40.

Jennings AE, Weiner NJ, Helgadottir G, et al. (2004) Modern foraminiferal faunas of the southwestern to northern Iceland shelf: oceanographic and environmental controls. *The Journal of Foraminiferal Research* 34: 180-207.

Jensen KG, Kuijpers A, Koç N, et al. (2004) Diatom evidence of hydrographic changes and ice conditions in Igaliku Fjord, South Greenland, during the past 1500 years. *The Holocene* 14: 152-164.

Jiang H, Seidenkrantz MS, Knudsen KL, et al. (2002) Late-Holocene summer sea-surface temperatures based on a diatom record from the north Icelandic shelf. *The Holocene* 12: 137-147.

Joughin I, Abdalati W and Fahnestock M. (2004) Large fluctuations in speed on Greenland's Jakobshavn Isbrae glacier. *Nature* 432: 608-610.

Kaneko M, Shingai H, Pohlman JW, et al. (2010) Chemical and isotopic signature of bulk organic matter and hydrocarbon biomarkers within mid-slope accretionary sediments of the northern Cascadia margin gas hydrate system. *Marine Geology* 275: 166-177.

Kaplan M. (2002) Holocene Environmental Variability in Southern Greenland Inferred from Lake Sediments. *Quaternary Research* 58: 149-159.

Kaufman D. (2004) Holocene thermal maximum in the western Arctic (0–180°W). *Quaternary Science Reviews* 23: 529-560.

Kelly M. (1980) *The status of the Neoglacial in western Greenland*: Grønlands geologiske undersøgelse.

Knudsen KL, Eiríksson J and Bartels-Jónsdóttir HB. (2012) Oceanographic changes through the last millennium off North Iceland: Temperature and salinity reconstructions based on foraminifera and stable isotopes. *Marine Micropaleontology* 84-85: 54-73.

Krawczyk D, Witkowski A, Moros M, et al. (2010) Late-Holocene diatom-inferred reconstruction of temperature variations of the West Greenland Current from Disko Bugt, central West Greenland. *The Holocene* 20: 659-666.

Kunz-Pirrung M. (2001) Dinoflagellate cyst assemblages in surface sediments of the Laptev Sea region (Arctic Ocean) and their relationship to hydrographic conditions. *Journal of Quaternary Science* 16: 637-649.

Lassen SJ, Kuijpers A, Kunzendorf H, et al. (2004) Late-Holocene Atlantic bottom-water variability in Igaliku Fjord, South Greenland, reconstructed from foraminifera faunas. *The Holocene* 14: 165-171.

Lloyd J. (2006a) Late Holocene environmental change in Disko Bugt, west Greenland: interaction between climate, ocean circulation and Jakobshavn Isbrae. *Boreas* 35: 35-49.

Lloyd J, Moros M, Perner K, et al. (2011) A 100 yr record of ocean temperature control on the stability of Jakobshavn Isbrae, West Greenland. *Geology* 39: 867-870.

Lloyd JM. (2006b) Modern Distribution of Benthic Foraminifera from Disko Bugt, West Greenland. *The Journal of Foraminiferal Research* 36: 315-331.

Lloyd JM, Kuijpers A, Long A, et al. (2007) Foraminiferal reconstruction of mid- to late-Holocene ocean circulation and climate variability in Disko Bugt, West Greenland. *The Holocene* 17: 1079-1091.

Lloyd JM, Park LA, Kuijpers A, et al. (2005) Early Holocene palaeoceanography and deglacial chronology of Disko Bugt, West Greenland. *Quaternary Science Reviews* 24: 1741-1755.

Long A and Roberts D. (2003) Late Weichselian deglacial history of Disko Bugt, West Greenland, and the dynamics of the Jakobshavns Isbrae ice stream. *Boreas* 32: 208-226.

Mackensen A, Rudolph M and Kuhn G. (2001) Late Pleistocene deep-water circulation in the subantarctic eastern Atlantic. *Global and Planetary Change* 30: 197-229.

Marret F and Scourse J. (2003) Control of modern dinoflagellate cyst distribution in the Irish and Celtic seas by seasonal stratification dynamics. *Marine Micropaleontology* 47: 101-116.

Matthews J. (1969) The assessment of a method for the determination of absolute pollen frequencies. *New Phytologist* 68: 161-166.

Matthiessen J, de Vernal A, Head M, et al. (2005) Modern organic-walled dinoflagellate cysts in arctic marine environments and their (paleo-) environmental significance. *Paläontologische Zeitschrift* 79: 3-51.

McCarthy D. (2011) Late Quaternary ice-ocean interactions in central West Greenland. Durham University.

McNeely R, Dyke AS and Southon JR. (2006) Canadian Marine Reservoir Ages, Preliminary Data Assessment. OpenFile 5049. *Geological Survey of Canada* 3.

Mertens KN, Verhoeven K, Verleye T, et al. (2009) Determining the absolute abundance of dinoflagellate cysts in recent marine sediments: The Lycopodium marker-grain method put to the test. *Review of Palaeobotany and Palynology* 157: 238-252.

Miller GH, Wolfe AP, Briner JP, et al. (2005) Holocene glaciation and climate evolution of Baffin Island, Arctic Canada. *Quaternary Science Reviews* 24: 1703-1721.

Moros M, Jensen KG and Kuijpers A. (2006) Mid- to late-Holocene hydrological and climatic variability in Disko Bugt, central West Greenland. *The Holocene* 16: 357-367.

Mudie P, Keen C, Hardy I, et al. (1984) Multivariate analysis and quantitative paleoecology of benthic foraminifera in surface and Late Quaternary shelf sediments, northern Canada. *Marine Micropaleontology* 8: 283-313.

Murray JW. (2006) *Ecology and applications of benthic foraminifera*: Cambridge University Press.

NODC (National Oceanographic Data Center). (2001) *World Ocean Database 2001, Scientific Data Sets, Observed and Standard Level Oceanographic Data.* National Oceanic and Atmospheric Administration, Boulder, Colorado.

NSIDC (National Snow and Ice Data Center). (2003) *Brightness temperature and ice concentrations grids for the polar regions.* NSIDC Distributed Active Archive Center, Boulder, Colorado.

Ó Cofaigh C, Dowdeswell JA, Jennings AE, et al. (2013) An extensive and dynamic ice sheet on the West Greenland shelf during the last glacial cycle. *Geology* 41: 219-222.

Ouellet-Bernier M-M. (2014) *Changements paléocéanographiques dans la région de Disko Bugt, Groenland, au cours de l'Holocène (Master thesis).* Université du Québec à Montréal.

Perner K, Moros M, Jennings A, et al. (2013) Holocene palaeoceanographic evolution off West Greenland. *The Holocene* 23: 374-387.

Perner K, Moros M, Lloyd JM, et al. (2011) Centennial scale benthic foraminiferal record of late Holocene oceanographic variability in Disko Bugt, West Greenland. *Quaternary Science Reviews* 30: 2815-2826.

Polyak L, Korsun S, Febo LA, et al. (2002) Benthic foraminiferal assemblages from the southern Kara Sea, a river-influenced Arctic marine environment. *The Journal of Foraminiferal Research* 32: 252-273.

Polyak L and Solheim A. (1994) Late□and postglacial environments in the northern Barents Sea west of Franz Josef Land. *Polar Research* 13: 197-207.

Potvin É, Rochon A, Lovejoy C, et al. (2013) Cyst-theca relationship of the arctic dinoflagellate cystIslandinium minutum(Dinophyceae) and phylogenetic position based on SSU rDNA and LSU rDNA. *Journal of Phycology*: n/a-n/a.

Radi T, Bonnet S, Cormier M-A, et al. (2013) Operational taxonomy and (paleo-) autecology of round, brown, spiny dinoflagellate cysts from the Quaternary of high northern latitudes. *Marine Micropaleontology* 98: 41-57.

Radi T and de Vernal A. (2008) Dinocysts as proxy of primary productivity in mid–high latitudes of the Northern Hemisphere. *Marine Micropaleontology* 68: 84-114.

Reimer PJ, Baillie MGL, Bard E, et al. (2009) IntCal09 and Marine09 radiocarbon age calibration curves, 0-50,000 years CAL BP. *Radiocarbon* 51: 1111-1150.

Ren J, Jiang H, Seidenkrantz M-S, et al. (2009) A diatom-based reconstruction of Early Holocene hydrographic and climatic change in a southwest Greenland fjord. *Marine Micropaleontology* 70: 166-176.

Ribeiro S, Moros M, Ellegaard M, et al. (2012) Climate variability in West Greenland during the past 1500 years: evidence from a high-resolution marine palynological record from Disko Bay. *Boreas* 41: 68-83.

Richerol T, Rochon A, Blasco S, et al. (2008) Evolution of paleo sea-surface conditions over the last 600 years in the Mackenzie Trough, Beaufort Sea (Canada). *Marine Micropaleontology* 68: 6-20.

Rignot E and Kanagaratnam P. (2006) Changes in the velocity structure of the Greenland Ice Sheet. *Science* 311: 986-990.

Roberts DH and Long AJ. (2005) Streamlined bedrock terrain and fast ice flow, Jakobshavns Isbrae, West Greenland: implications for ice stream and ice sheet dynamics. *Boreas* 34: 25-42.

Rochon A, Vernal Ad, Turon J-L, et al. (1999) Distribution of recent dinoflagellate cysts in surface sediments from the North Atlantic Ocean and adjacent seas in relation to sea-surface parameters. *American Association of Stratigraphic Palynologists Contribution Series* 35: 1-146.

Rytter F, Knudsen KL, Seidenkrantz M-S, et al. (2002) Modern distribution of benthic foraminifera on the North Icelandic shelf and slope. *The Journal of Foraminiferal Research* 32: 217-244.

Sangiorgi F, Capotondi L and Brinkhuis H. (2002) A centennial scale organic-walled dinoflagellate cyst record of the last deglaciation in the South Adriatic Sea (Central Mediterranean). *Palaeogeography, Palaeoclimatology, Palaeoecology* 186: 199-216.

Schafer CT and Cole FE. (1986) Reconnaissance survey of benthonic foraminifera from Baffin Island fiord environments. *Arctic* 39: 232-239.

Seidenkrantz M-S, Ebbesen H, Aagaard-Sørensen S, et al. (2013) Early Holocene large-scale meltwater discharge from Greenland documented by foraminifera and sediment parameters. *Palaeogeography, Palaeoclimatology, Palaeoecology* 391: 71-81.

Seidenkrantz M-S, Roncaglia L, Fischel A, et al. (2008) Variable North Atlantic climate seesaw patterns documented by a late Holocene marine record from Disko Bugt, West Greenland. *Marine Micropaleontology* 68: 66-83.

Seidenkrantz MS, Aagaard-Sorensen S, Sulsbruck H, et al. (2007) Hydrography and climate of the last 4400 years in a SW Greenland fjord: implications for Labrador Sea palaeoceanography. *The Holocene* 17: 387-401.

St□Onge MP and St□Onge G. (2014) Environmental changes in Baffin Bay during the Holocene based on the physical and magnetic properties of sediment cores. *Journal of Quaternary Science* 29: 41-56.

Steinsund P. (1994) Benthic foraminifera in surface sediments of the Barents and Kara seas: modern and late Quaternary applications. *Unpublished PhD thesis, University of Tromsø, Norway.*

Stuiver M and Reimer PJ. (1993) Extended 14C data base and revised CALIB 3.0 14C age calibration program. *Radiocarbon* 35: 215-230.

Tang CCL, Ross CK, Yao T, et al. (2004) The circulation, water masses and sea-ice of Baffin Bay. *Progress in Oceanography* 63: 183-228.

Verhoeven K, Louwye S, Paez-Reyes M, et al. (2014) New acritarchs from the late Cenozoic of the southern North Sea Basin and the North Atlantic realm. *Palynology*: 1-13.

Vinther BM, Clausen HB, Johnsen SJ, et al. (2006) A synchronized dating of three Greenland ice cores throughout the Holocene. *Journal of Geophysical Research: Atmospheres (1984–2012)* 111.

Weidick A. (1992) Jakobshavn Isbræ area during the climatic optimum. *Rapport Grønlands Geologiske Undersøgelse* 155: 67-72.

Weidick A and Bennike O. (2007) Quaternary glaciation history and glaciology of Jakobshavn Isbræ and the Disko Bugt region, West Greenland: A review. 1-78.

Weidick A, Oerter H, Reeh N, et al. (1990) The recession of the Inland Ice margin during the Holocene climatic optimum in the Jakobshavn Isfjord area of West Greenland. *Global and Planetary Change* 2: 389-399.

Wollenburg JE and Mackensen A. (1998) Living benthic foraminifers from the central Arctic Ocean: faunal composition, standing stock and diversity. *Marine Micropaleontology* 34: 153-185.

Young NE, Briner JP, Stewart HAM, et al. (2011) Response of Jakobshavn Isbrae, Greenland, to Holocene climate change. *Geology* 39: 131-134.

Zonneveld KA, P Hoek R, Brinkhuis H, et al. (2001) Geographical distributions of organic-walled dinoflagellate cysts in surficial sediments of the Benguela upwelling region and their relationship to upper ocean conditions. *Progress in Oceanography* 48: 25-72.

Table 1.1 Radiocarbon dates for core MSM343300. Calibrated years include one standard deviation

Depths (cm)	Lab. code	Material	Mass (mg C)	^{14}C date (yr BP)	Calibrated yr BP 1950 ΔR 140±35	Median
5.5	Poz-39052	Mix benthic foraminifera	0.3	1415 ± 35	767-885	826
30	Poz-39051	Mix benthic foraminifera	0.4	1645 ± 30	990-1117	1053.5
71	Poz-33489	Mix benthic foraminifera		1990 ± 50	1324-1466	1395
100.5	Poz-39047	Mix benthic foraminifera		2305 ± 30	1697-1817	1757
149.5	Poz-39048	Mix benthic foraminifera	0.35	2750 ± 60	2167-2353	2260
169.5	Poz-43445	Mix benthic foraminifera	0.7	3005 ± 35	2561-2713	2637
190	AA-81304	Paired *Yoldia limatula*		3248 ± 44	2800-2935	2867.5
213.5	Poz-30985	*G. auriculata arctica & N. labradorica*		3715 ± 35	3401-3532	3466.5
219.5	Poz-43446	Mix benthic foraminifera	0.3	3820 ± 50	3507-3675	3591
239.5	Poz-43447	Mix benthic foraminifera	0.2	4410 ± 50	4290-4474	4382
261.5	Poz-33456	*G. auriculata arctica & N. labradorica*		4490 ± 40	4410-4555	4482.5
297.5	Poz-33457	*N. labradorica*		4970 ± 40	5041-5226	5133.5
319.5	Poz-39053	Mix benthic foraminifera		5440 ± 40	5594-5708	5651
340	AA-81307	*G. auriculata arctica & N. labradorica*		5822 ± 57	6000-6171	6085.5
359	Poz-39054	Mix benthic foraminifera	0.4	6500 ± 50	6746-6905	6825.5
381	LuS 9918	Mix benthic foraminifera		6380 ± 80	6575-6795	6685
399.5	Poz-39055	Mix benthic foraminifera		7390 ± 50	7649-7782	7715.5
434	LuS 9704	Mix benthic foraminifera	0.27	7025 ± 70	7318-7466	7392
456	LuS 9919	Mix benthic foraminifera		7780 ± 80	7995-8184	8089.5
541.5	LuS 9705	Mix benthic foraminifera	0.37	8585 ± 75	8967-9194	9080.5
597.5	Poz-33458	Unid gastropod		9390 ± 60	9994-10176	10085
655	AA-81305	Paired *Yoldia*. chalky		9473 ± 57	10106-10250	10178
668	LuS 9706	Mix benthic foraminifera	0.34	9475 ± 80	10068-10292	10180
976.5	LuS 9707	Mix benthic foraminifera	0.43	9295 ± 80	9810-10109	9959.5
1113	LuS 9708	Mix benthic foraminifera	0.25	9455 ± 90	10000-10261	10130.5

Poz - Poznan Radiocarbon Laboratory
AA - Aarhus University
LuS - Lund University

Table 1.2 List of dinoflagellate cysts

	Dinoflagellate cyst names		References
	Islandinium minutum	H	(Harland and Reid in Harland et al., 1980)
	Islandinium ? *cezare*	H	(de Vernal et al., 1989 ex de Vernal *in* Rochon et al., 1999) Radi et al., 2013
	Echinidinium karaense	H	(Head et al., 2001) Radi et al., 2013
	Selenopemphix quanta	H	(Bradford, 1975) Matsuoka, 1985
	Brigantedinium spp.	H	Reid, 1977 ex Lentin and Williams, 1993
Grouped as *Brigantedinium* spp.	*Brigantedinium simplex*	H	Wall 1965 ex Lentin and Williams, 1993
Grouped as *Brigantedinium* spp.	*Brigantedinium cariacoense*	H	(Wall, 1967) Lentin and Williams, 1993
	Operculodinium centrocarpum sensu	A	Wall and Dale, 1966
Grouped as *Operculodinium centrocarpum* sensu	*Operculodinium centrocarpum* short processes	A	Wall and Dale, 1966
Grouped as *Operculodinium centrocarpum* sensu	*Operculodinium centrocarpum* Arctic	A	
	Nematosphaeropsis labyrinthus	A	(Ostenfeld, 1903) Reid, 1974
	Spiniferites elongatus	A	Reid, 1974
	Spiniferites ramosus	A	(Ehrenberg, 1838) Mantell, 1854 sensu lato
	Spiniferites spp.	A	
	Cyst of *Pentapharsodinium dalei*	A	Indelicato & Loeblich III, 1986

H=Heterotrophic, A=Autotrophic

Figure 1.1 Map of the study area

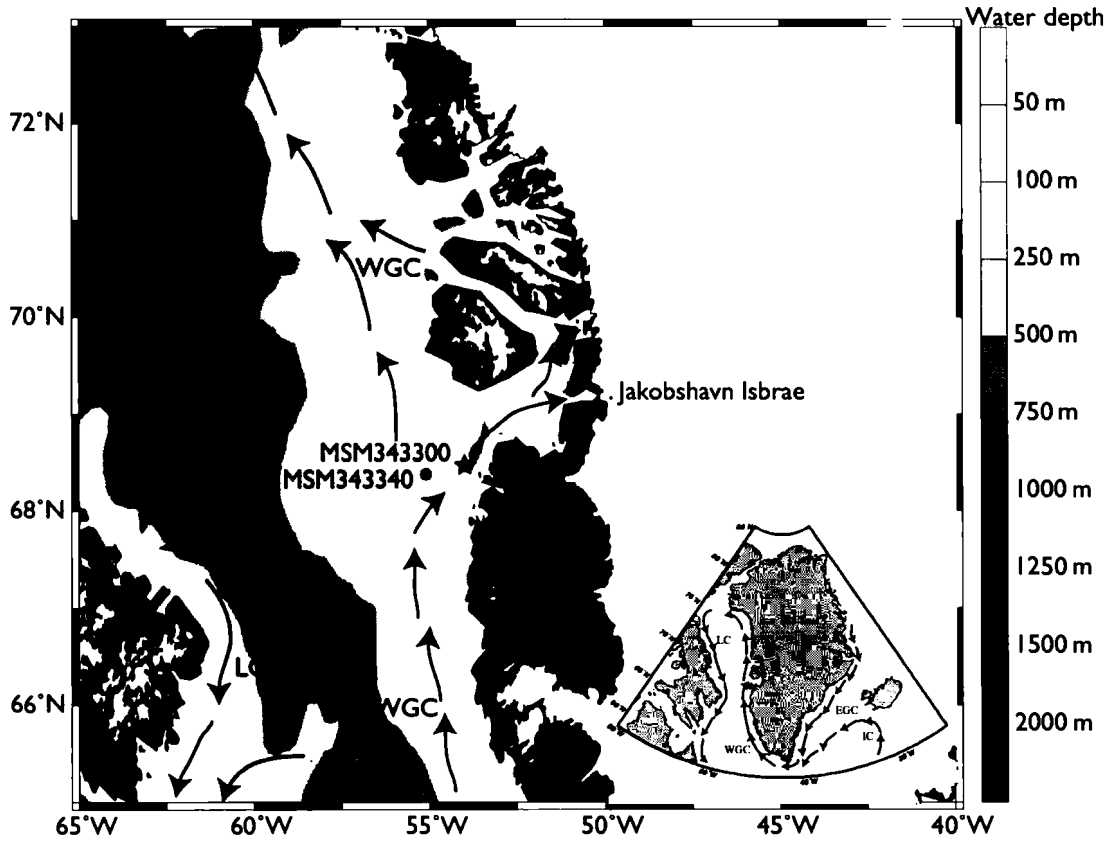

Location of the studied core MSM343300, indicated by a star, and the nearby core MSM343340 also discussed here (round dot). EGC: East Greenland Current, WGC: West Greenland Current, IC: Irminger Current, LC: Labrador Current.

Figure 1.2 Age vs. depth relationship in core MSM343300

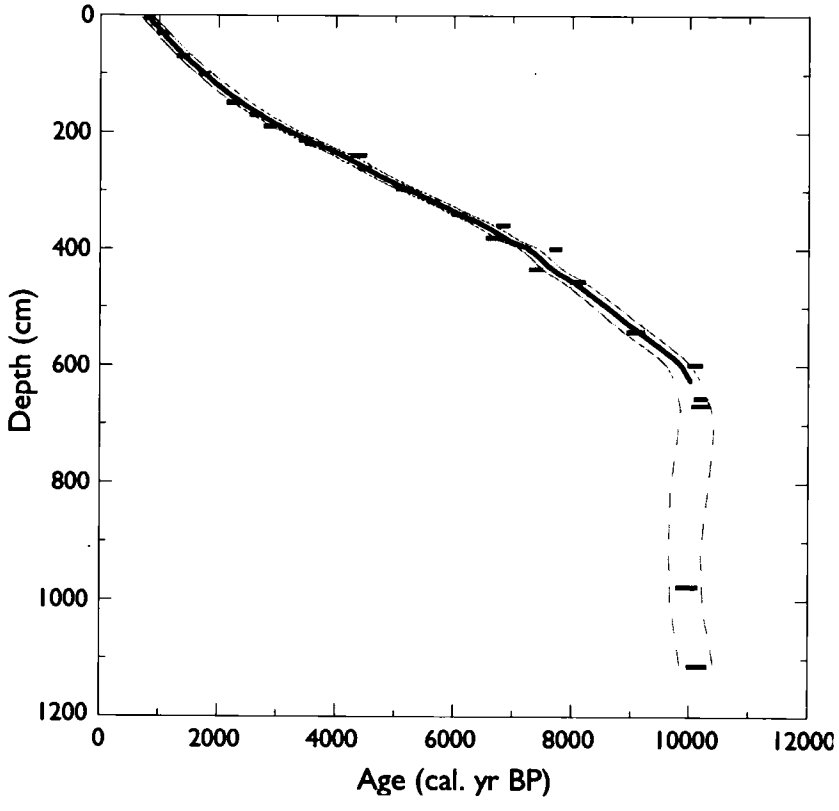

1-sigma range calibrated age 14 C is represented in black, smooth interpolation on the median values is represented by a black line and 2-sigma range smooth interpolations are represented by a gray line.

Figure 1.3 Percentages of main dinocyst taxa in core MSM343300 and concentrations of dinocyst, pollen grains, *Halodinium* and organic linings of foraminifers.

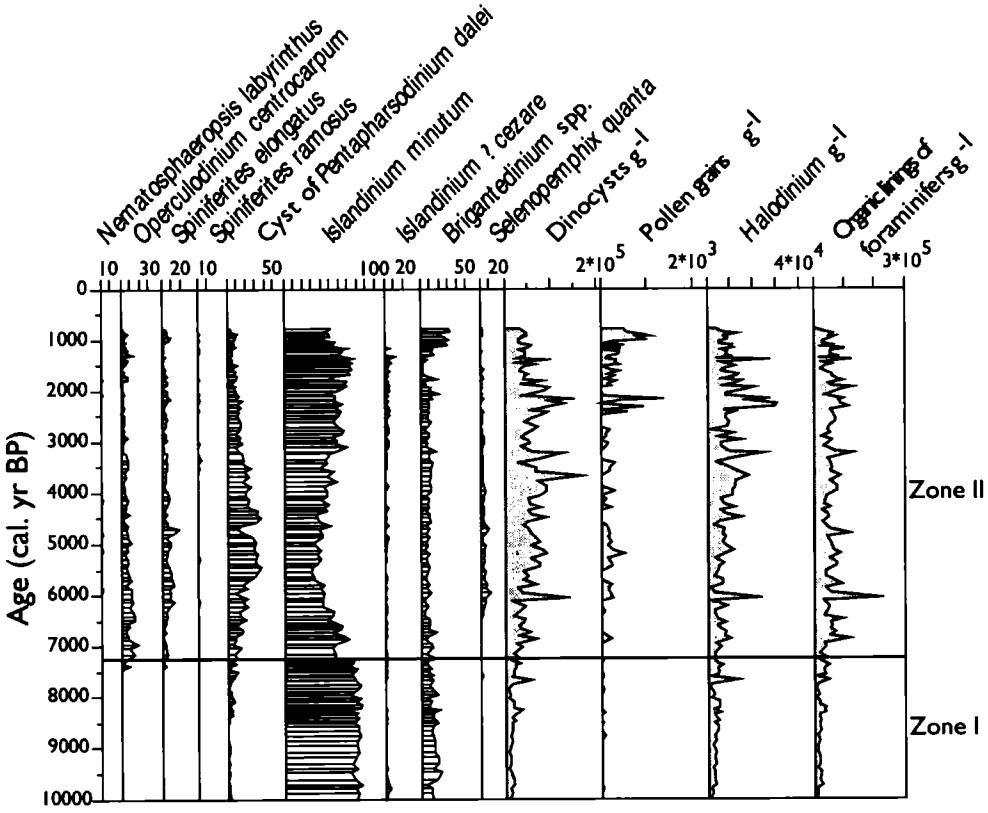

Figure 1.4 Reconstruction of summer sea-surface temperature (SST), salinity (SSS), seasonal sea ice cover in months.yr^{-1} and productivity (in gC m^{-2}.yr^{-1}) for the last ~10 000 years based on MAT applied to dinocyst assemblages in core MSM343300.

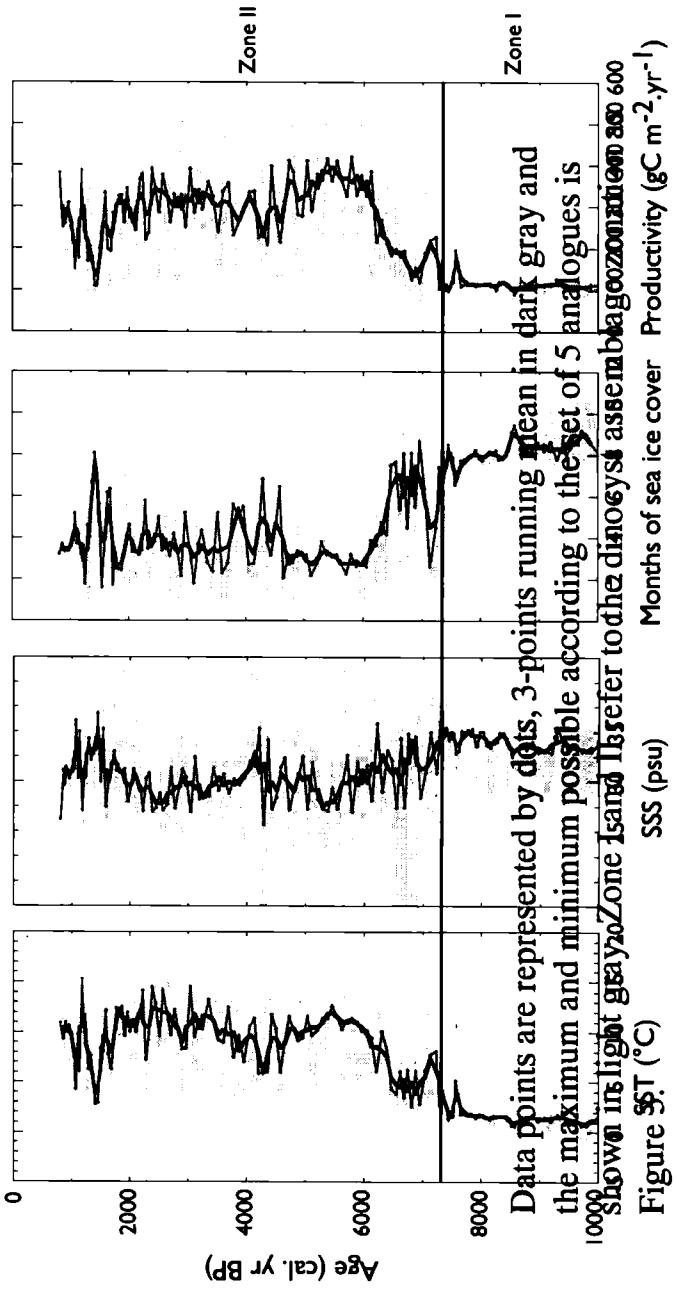

Data points are represented by dots, 3-points running mean in dark gray and the maximum and minimum possible according to the set of 5 analogues is shown in light gray. Zone I and II refer to the dinocyst assemblage zonation

Figure 3.

Figure 1.5 Isotopic compositions ($\delta^{13}C$ and $\delta^{18}O$) of *Islandiella norcrossi* (solid diamonds) and *Nonionellina labradorica* (circles) from core MSM343300

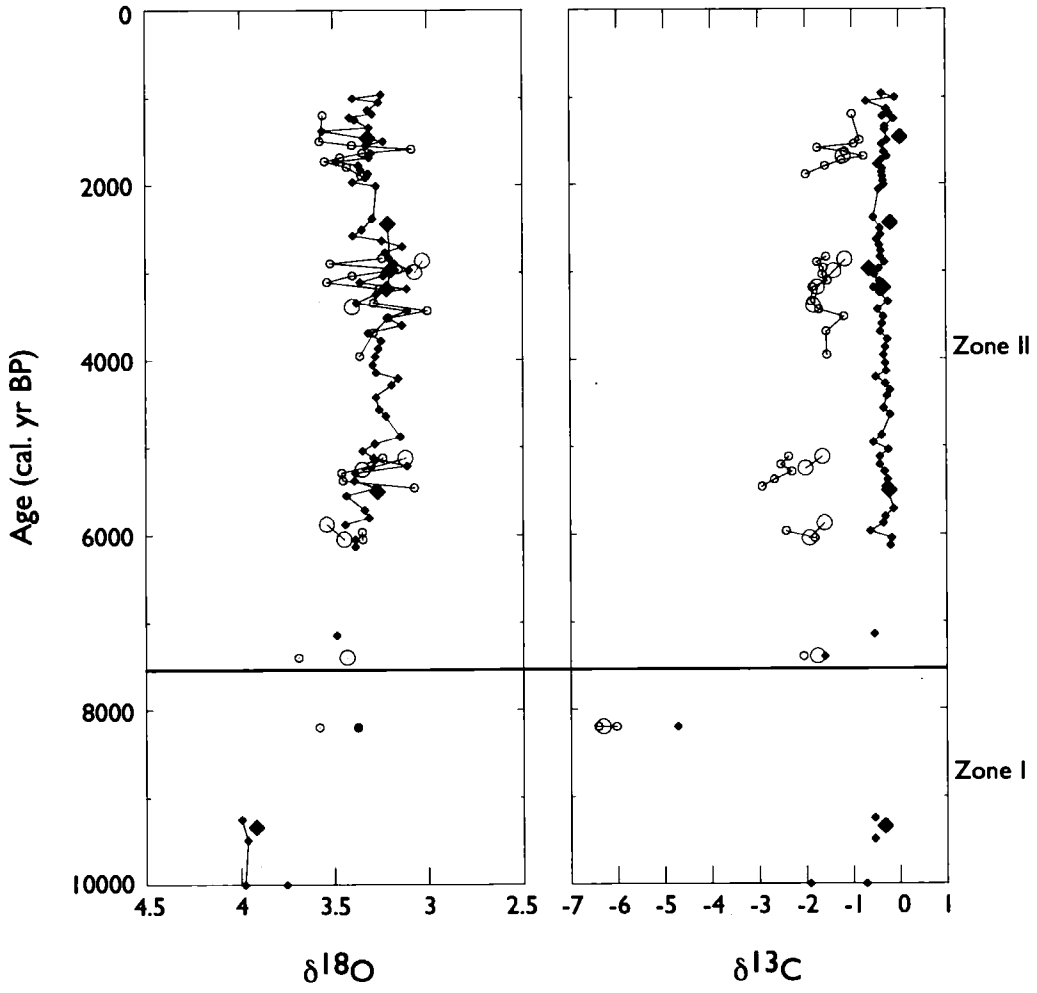

Larger and smaller symbols correspond to the larger (>250 μm) and smaller (150-250 μm) size range of analyzed specimens. Zone I and II refer to the dinocyst assemblage zonation as Figure 3.

Figure 1.6a Comparison of sea-surface temperature from core MSM343300 (this study) with reconstruction from adjacent marine cores of southwest and west Greenland, and with the NGRIP $\delta^{18}O$ record (Vinther *et al.*, 2006) (graphic representation)

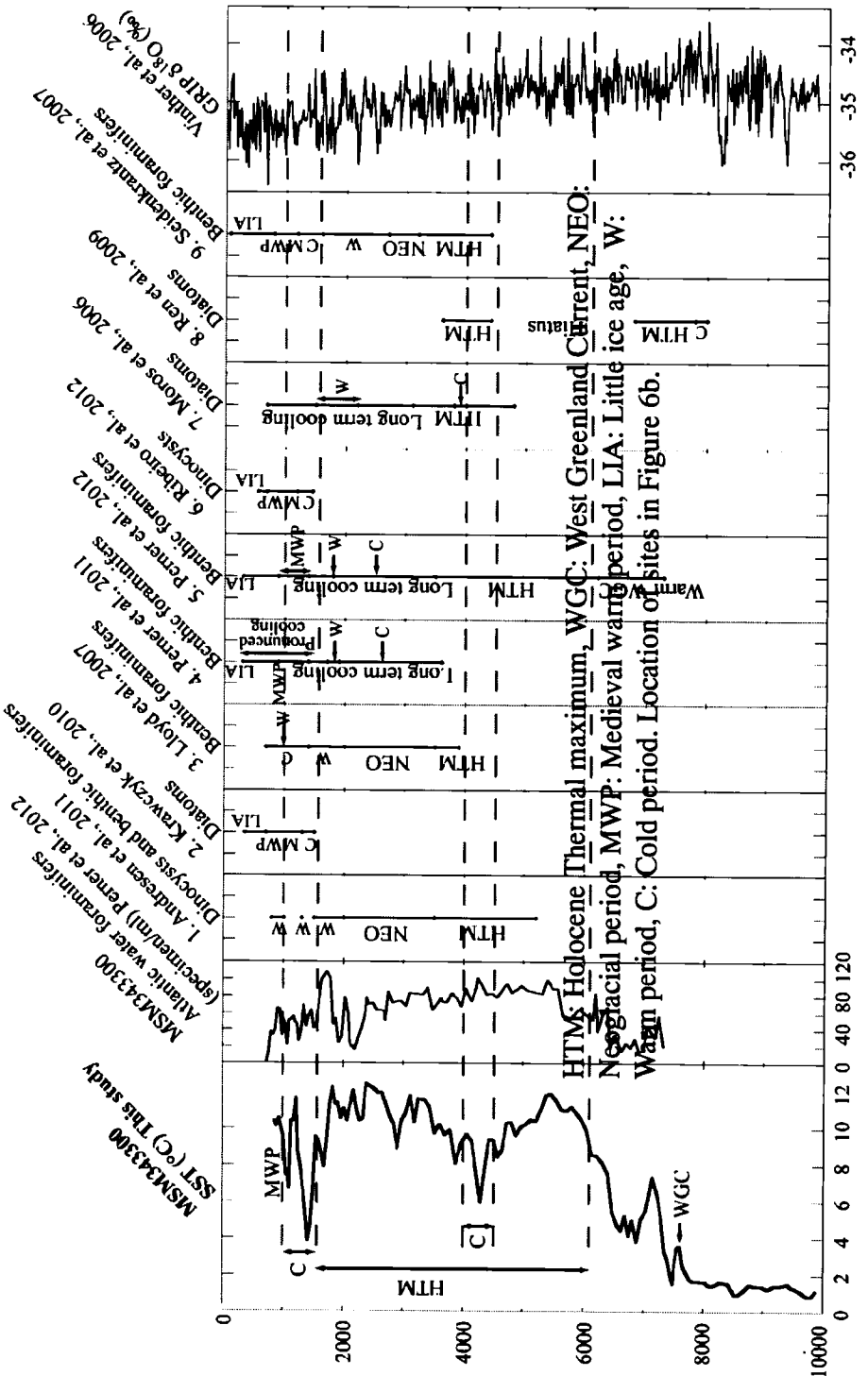

Figure 1.6b **Map of the sites referred to by the numbers in of Figure 6a**

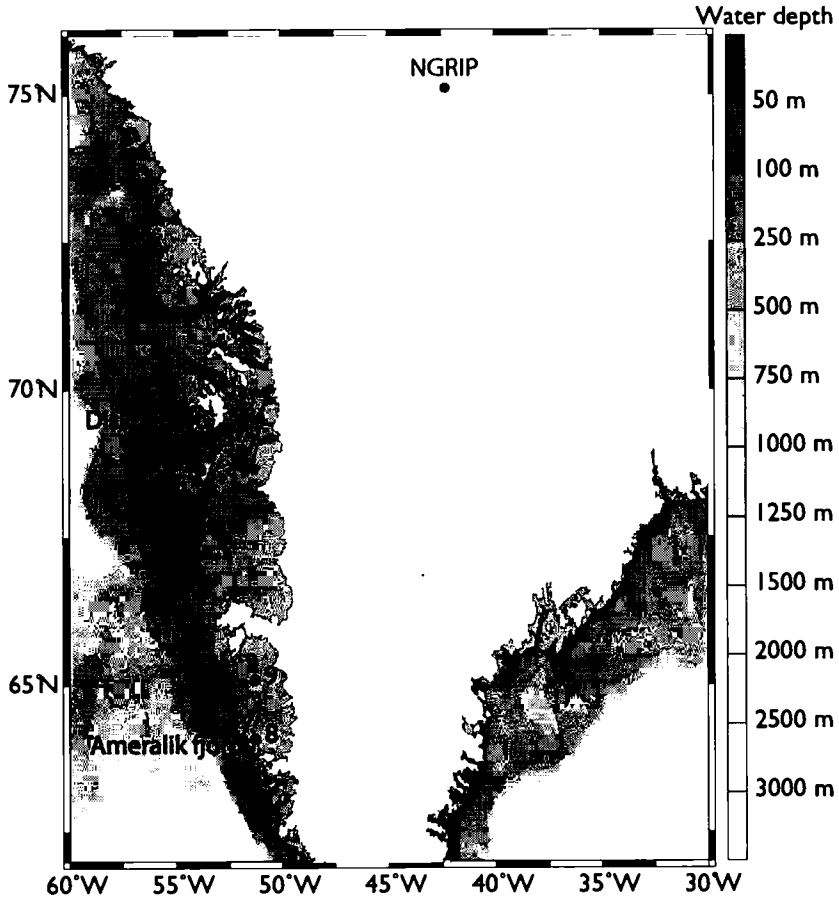

CONCLUSION

Les analyses micropaléontologiques de la carotte MSM343300 ont permis d'établir une reconstitution climatique et paléocéanographique de la région de Disko Bugt au cours des derniers ~10 000 ans. D'une part, la technique des analogues modernes a permis une reconstitution de la température et de la salinité à partir des assemblages de kystes de dinoflagellé, démontrant ainsi la pertinence du proxy pour la paléocéanographie de milieux arctiques et subarctiques. La reconstitution des deux paramètres clés, température et salinité, permet d'affirmer que les eaux de surface sont influencées localement par les apports d'eaux de fonte du glacier Jakobshavn Isbrae et/ou des marges groenlandaises. En effet, une augmentation des températures est associée à une diminution de la salinité et vice-versa. D'autre part, les analyses isotopiques des foraminifères benthiques ont permis une meilleure compréhension de l'évolution des courants, à quelques centaines de mètres de profondeur.

Aux environs de 10 000 ans cal. BP, la marge glaciaire se stabilise sur le plateau continental pendant près de 1000 ans (McCarthy, 2011). La première manifestation du Courant ouest-groenlandais s'est faite en profondeur vers ~10 000 ans cal. BP lorsque le foraminifère benthique *Islandiella norcrossi* colonise la région. En surface, le couvert de glace de mer était quasi-continu et la température était très basse. L'établissement de conditions postglaciaires marquées par une augmentation des températures de surface s'est fait à partir de ~7300 ans cal. BP, lorsque le Courant ouest-groenlandais circule en surface amenant une augmentation de la diversité des espèces dans les assemblages de dinokystes. Ce sont les apports de fonte en provenant du glacier Jakobshavn Isbrae qui auraient retardé l'établissement de conditions de surface postglaciaires, une faible salinité de surface engendrant la

subduction du Courant ouest-groenlandais (e.g. Ren *et al.*, 2009 ; Seidenkrantz *et al.*, 2013). Un optimum thermique est enregistré à partir de ~6000 ans cal. BP lorsque la contribution des eaux atlantiques est devenue dominante à la surface. De courtes périodes de refroidissement sont observées, de ~4200-4000 et de ~1500-1000 ans cal. BP, pendant lesquelles le Courant ouest-groenlandais paraît avoir été surtout influencé par les eaux polaires. Finalement, des températures maximales, nettement plus élevées qu'à l'actuel, sont enregistrées de ~1000 à ~800 ans cal. BP ce qui correspondrait à la période chaude médiévale.

APPENDICE A

RESULTATS DES DINOKYSTES ET AUTRES PALYNOMORPHES

Tableau A.1 : Dénombrements et concentrations des dinokystes dans la carotte MSM343300

Tableau A.2 : Dénombrements et concentrations des grains de pollens et autres palynomorphes dans la carotte MSM343300

Tableau A.3 : Reconstitution des conditions de surface à partir des abondances relatives des dinokystes de la carotte MSM343300 en utilisant la méthode des analogues modernes (Base de données du Geotop; n=1492)

Figure A.1 : Abondances relatives des dinokystes et concentrations des principaux palynomorphes

Figure A.2 : Reconstitutions de surface de la température, salinité, couvert de glace et productivité de la carotte MSM343300 en utilisant la méthode des analogues modernes (Base de données du Geotop n=1492)

Figure A.3 : Analyse en composantes principales réalisée à partir des abondances relatives des dinokystes de la carotte MSM343300

Tableau A.1 Dénombrements et concentrations des dinokystes dans la carotte MSM343300

Profondeur (cm)	**3**	**9**	**13**	**17**	**20**	**25**	**30**	**33**	**37**	**40**	**45**	**49**
Poids sec (g)	2,912	3,656	2,547	3,569	3,654	3,150	2,938	3,328	3,100	2,614	5,930	6,029
Volume (ml)	1,5	2,0	1,5	2,0	2,0	2,0	2,0	2,0	2,0	1,5	3,0	3,0
Nombre de *L. clavatum*/capsule	18583	18583	18583	18583	18583	18583	18583	18583	18583	18583	18583	18583
Lycopodium clavatum ajoutés	89	36	51	45	37	59	66	48	35	40	20	27
Nematosphaeropsis labyrinthus	1	1	5	1	3	4	6	4	5	4	1	2
Operculodinium centrocarpum	10	14	26	14	18	10	20	13	14	19	19	25
Spiniferites elongatus	19	23	17	29	36	26	15	5	9	11	4	10
Spiniferites ramosus	7	4	7	3	6	7	2	1	4	2	9	9
Spiniferites spp.	0	3	2	1	0	2	2	0	3	0	0	3
Cyst of *Pentapharsodinium dalei*	23	13	41	24	33	26	14	25	24	32	19	21
Islandinium minutum	239	149	170	179	150	142	189	178	193	179	224	190
Islandinium ? cezare	0	0	0	0	1	0	0	0	0	0	21	0
Brigantedinium spp.	151	106	67	82	89	101	84	90	105	60	19	44
Selenopemphix quanta	14	6	8	12	6	2	2	0	2	1	5	5
Somme des dinokystes	**464**	**319**	**343**	**345**	**342**	**320**	**334**	**316**	**359**	**308**	**321**	**309**
Dinokystes/g	33271	45045	49064	39922	47003	31994	32010	36760	61485	54748	50301	35273
Dinokystes (cm^2/an)	5296	6751	6832	5841	7042	4132	3856	5016	7815	7822	8152	5813

Profondeur (cm)	**52**	**57**	**61**	**65**	**69**	**73**	**77**	**81**	**85**	**89**	**93**	**97**
Poids sec (g)	3,128	3,708	3,974	4,106	3,454	3,375	3,610	3,723	3,109	3,067	4,161	4,616
Volume (ml)	2,0	2,0	2,0	2,0	2,0	2,0	2,0	2,0	2,0	2,0	2,0	2,0
Nombre de *L. clavatum*/capsule	18583	18583	18583	18583	18583	18583	18583	18583	18583	18583	18583	18583
Lycopodium clavatum ajoutés	41	40	30	48	16	52	25	34	56	58	27	25
Nematosphaeropsis labyrinthus	4	1	2	0	0	2	0	2	0	0	0	2
Operculodinium centrocarpum	15	50	10	14	24	23	16	9	5	15	11	24
Spiniferites elongatus	11	2	11	9	8	5	12	9	17	11	15	17
Spiniferites ramosus	7	5	2	2	1	0	4	3	4	2	2	4
Spiniferites spp.	2	0	0	0	0	0	0	1	1	0	0	0
Cyst of *Pentapharsodinium dalei*	18	22	14	17	22	17	40	25	22	29	28	33
Islandinium minutum	207	226	203	251	209	251	227	229	234	224	227	162
Islandinium ? cezare	5	4	37	18	16	26	18	16	8	18	10	13
Brigantedinium spp.	40	60	19	11	27	10	9	9	7	11	12	17
Selenopemphix quanta	8	2	4	4	0	2	5	5	14	6	4	8
Somme des dinokystes	**317**	**372**	**302**	**326**	**307**	**336**	**331**	**308**	**312**	**316**	**309**	**280**
Dinokystes/g	45931	46613	47070	30736	103234	35579	68160	45215	33298	33014	51116	45090
Dinokystes (cm^2/an)	5891	7086	7670	5175	14619	4923	10088	6902	4245	4151	8720	8533

Profondeur (cm)	**101**	**105**	**109**	**113**	**117**	**121**	**125**	**129**	**134**	**137**	**141**	**145**
Poids sec (g)	4,775	4,036	3,786	2,850	3,736	3,184	2,784	3,658	2,653	2,930	2,819	4,480
Volume (ml)	2,0	2,0	2,0	2,0	2,0	2,0	1,0	2,0	1,5	1,5	2,0	2,0
Nombre de *L. clavatum*/capsule	18583	18583	18583	18583	18583	18583	18583	18583	18583	18583	18583	18583
Lycopodium clavatum ajoutés	29	13	32	26	15	20	36	34	15	20	15	13
Nematosphaeropsis labyrinthus	6	1	1	1	0	1	6	1	2	0	0	2
Operculodinium centrocarpum	29	4	11	10	6	11	15	10	11	11	8	13
Spiniferites elongatus	10	16	21	9	4	20	23	19	31	18	14	10
Spiniferites ramosus	7	2	3	1	1	1	11	3	7	7	3	4
Spiniferites spp.	5	4	4	3	8	6	9	9	6	4	0	0
Cyst of *Pentapharsodinium dalei*	32	22	16	34	25	30	37	40	25	53	37	48
Islandinium minutum	160	169	205	219	201	178	148	173	189	176	196	173
Islandinium ? cezare	0	11	15	18	14	22	0	14	4	15	11	16
Brigantedinium spp.	62	10	20	14	33	29	66	32	43	26	32	30
Selenopemphix quanta	13	4	9	4	10	5	7	1	16	8	5	5
Somme des dinokystes	**324**	**243**	**305**	**313**	**302**	**303**	**322**	**302**	**334**	**318**	**306**	**301**
Dinokystes/g	43485	86067	46789	78484	100139	88427	59712	45122	155944	100857	134464	96033
Dinokystes (cm^2/an)	8512	14242	7262	9172	15340	11543	13630	6767	22620	16152	15543	17641

Profondeur (cm)	**149**	**153**	**157**	**161**	**165**	**169**	**174**	**177**	**181**	**185**	**189**	**193**
Poids sec (g)	3,217	2,675	3,247	3,352	4,543	3,518	3,591	3,281	3,923	3,569	4,064	3,358
Volume (ml)	1,5	1,5	2,0	1,5	2,0	2,0	2,0	1,5	2,0	2,0	2,0	2,0
Nombre de *L. clavatum*/capsule	18583	18583	18583	18583	18583	18583	18583	18583	18583	18583	18583	18583
Lycopodium clavatum ajoutés	15	23	22	29	28	22	25	49	41	34	28	47
Nematosphaeropsis labyrinthus	0	0	0	0	0	2	0	1	4	1	0	2
Operculodinium centrocarpum	5	5	14	16	12	9	15	9	26	15	12	7
Spiniferites elongatus	3	13	15	17	14	15	3	17	15	24	4	11
Spiniferites ramosus	4	5	1	5	3	1	4	5	2	2	11	4
Spiniferites spp.	1	0	3	5	1	4	2	0	0	0	2	0
Cyst of *Pentapharsodinium dalei*	20	42	35	39	52	51	42	44	54	47	59	32
Islandinium minutum	103	196	188	177	178	192	205	268	176	212	190	222
Islandinium ? cezare	9	12	19	11	9	14	13	15	5	14	17	12
Brigantedinium spp.	13	30	24	27	39	23	15	38	32	25	26	19
Selenopemphix quanta	5	12	11	9	11	4	7	13	16	14	14	11
Somme des dinokystes	**163**	**315**	**310**	**306**	**319**	**315**	**306**	**410**	**330**	**354**	**335**	**320**
Dinokystes/g	62781	95135	80637	58490	46602	75632	63348	47391	38128	54209	54710	37681
Dinokystes (cm^2/an)	11039	13913	10736	6536	5293	6652	5686	5183	3739	4837	5558	3163

Profondeur (cm)	**197**	**200**	**205**	**209**	**213**	**217**	**221**	**225**	**229**	**233**	**237**	**241**
Poids sec (g)	4,125	3,750	3,778	4,004	4,006	3,849	3,053	4,188	3,758	3,458	2,763	3,714
Volume (ml)	2,0	2,0	2,0	2,0	2,0	2,0	2,0	2,0	2,0	2,0	1,5	2,0
Nombre de *L. clavatum*/capsule	18583	18583	18583	18583	18583	18583	18583	18583	18583	18583	18583	18583
Lycopodium clavatum ajoutés	23	12	20	45	24	23	11	23	17	18	27	35
Nematosphaeropsis labyrinthus	0	1	2	2	1	2	2	1	1	1	2	7
Operculodinium centrocarpum	9	18	27	24	31	14	19	13	15	14	19	29
Spiniferites elongatus	9	23	16	19	20	12	13	20	11	21	28	28
Spiniferites ramosus	4	5	12	3	7	3	5	2	3	0	3	3
Spiniferites spp.	0	0	1	1	0	0	1	0	0	0	4	2
Cyst of *Pentapharsodinium dalei*	43	57	59	53	97	60	74	64	85	65	64	89
Islandinium minutum	175	165	141	158	143	178	148	223	144	150	149	149
Islandinium ? cezare	4	7	6	6	13	4	4	5	13	1	4	2
Brigantedinium spp.	51	33	31	46	41	39	34	39	35	37	22	33
Selenopemphix quanta	9	11	9	11	9	8	10	11	12	20	17	17
Somme des dinokystes	**304**	**320**	**304**	**323**	**362**	**320**	**310**	**378**	**319**	**309**	**312**	**359**
Dinokystes/g	59543	132142	74759	33315	69970	67181	171543	72931	92797	92250	77710	51324
Dinokystes (cm^2/an)	6140	12389	7062	3335	7007	6464	13093	7635	8718	7975	7158	4765

Profondeur (cm)	**245**	**249**	**253**	**257**	**261**	**265**	**269**	**273**	**277**	**281**	**285**	**289**
Poids sec (g)	3,169	3,302	2,919	3,733	3,096	3,747	4,131	2,598	3,958	3,098	3,449	4,050
Volume (ml)	1,5	1,5	1,5	2,0	2,0	2,0	2,0	1,5	2,0	1,5	1,5	2,0
Nombre de *L. clavatum*/capsule	18583	18583	18583	18583	18583	18583	18583	18583	18583	18583	18583	18583
Lycopodium clavatum ajoutés	36	23	39	32	22	31	36	42	25	33	24	28
Nematosphaeropsis labyrinthus	4	2	3	4	1	1	5	3	7	4	6	4
Operculodinium centrocarpum	25	20	12	35	11	16	25	20	26	27	38	23
Spiniferites elongatus	25	16	9	21	12	17	19	59	37	16	33	34
Spiniferites ramosus	0	0	0	2	3	0	3	4	4	1	2	3
Spiniferites spp.	0	0	1	0	1	0	0	0	0	0	0	0
Cyst of *Pentapharsodinium dalei*	77	84	108	116	127	97	54	39	64	101	108	104
Islandinium minutum	171	151	155	125	125	126	178	123	136	155	118	127
Islandinium ? cezare	6	13	7	6	12	5	14	3	2	14	12	9
Brigantedinium spp.	30	36	18	36	34	37	22	34	18	35	19	32
Selenopemphix quanta	9	18	12	15	10	12	20	31	23	11	10	21
Somme des dinokystes	**347**	**340**	**325**	**360**	**336**	**311**	**340**	**316**	**317**	**364**	**346**	**357**
Dinokystes/g	56517	83186	53054	55997	91668	49752	42490	53808	59535	66166	77687	58509
Dinokystes (cm^2/an)	5971	9157	5162	5226	7095	4661	4388	4660	5891	6833	8930	5923

Profondeur (cm)	**293**	**297**	**301**	**305**	**309**	**313**	**317**	**321**	**325**	**329**	**333**	**337**
Poids sec (g)	4,302	3,918	4,285	3,989	4,361	3,911	4,218	4,163	4,839	4,333	5,513	4,778
Volume (ml)	2,0	2,0	2,0	2,0	2,0	2,0	2,0	2,0	2,0	2,0	2,0	2,0
Nombre de *L. clavatum*/capsule	18583	18583	18583	18583	18583	18583	18583	18583	18583	18583	18583	18583
Lycopodium clavatum ajoutés	15	18	25	21	19	34	26	32	16	49	16	14
Nematosphaeropsis labyrinthus	6	3	2	4	5	4	4	4	5	7	1	3
Operculodinium centrocarpum	27	17	26	31	21	24	31	37	12	37	22	60
Spiniferites elongatus	19	24	15	25	28	28	29	36	38	29	18	40
Spiniferites ramosus	4	2	7	3	2	5	1	5	2	5	2	2
Spiniferites spp.	0	0	0	0	1	0	0	1	0	1	0	4
Cyst of *Pentapharsodinium dalei*	91	117	107	114	129	100	92	76	53	74	15	112
Islandinium minutum	121	129	138	131	110	93	101	105	128	138	77	222
Islandinium ? cezare	8	5	7	1	5	4	9	8	2	7	1	10
Brigantedinium spp.	12	35	25	30	34	23	19	21	29	19	19	29
Selenopemphix quanta	14	19	17	16	10	21	16	12	23	19	19	30
Somme des dinokystes	**302**	**351**	**344**	**355**	**345**	**302**	**302**	**305**	**292**	**336**	**174**	**512**
Dinokystes/g	86960	92488	59677	78762	77369	42200	51179	42548	70083	29408	36655	142252
Dinokystes (cm^2/an)	9353	9059	6393	7854	8436	4127	5396	4428	8478	3186	5052	16990

Profondeur (cm)	**341**	**345**	**349**	**353**	**357**	**361**	**365**	**369**	**373**	**377**	**381**	**385**
Poids sec (g)	5,946	4,073	5,516	5,138	5,971	3,760	5,500	3,415	3,616	5,003	4,913	4,682
Volume (ml)	2,5	2,0	2,5	2,0	3,0	1,5	2,0	1,5	1,5	2,0	1,5	2,0
Nombre de *L. clavatum*/capsule	18583	18583	18583	18583	18583	18583	18583	18583	18583	18583	18583	18583
Lycopodium clavatum ajoutés	47	35	32	45	21	34	32	36	27	32	16	51
Nematosphaeropsis labyrinthus	4	5	0	1	1	1	0	0	0	0	0	0
Operculodinium centrocarpum	43	38	43	40	46	27	32	16	20	27	28	66
Spiniferites elongatus	42	28	18	18	12	11	8	6	11	5	7	15
Spiniferites ramosus	7	0	3	2	0	0	1	0	4	0	2	0
Spiniferites spp.	0	1	2	0	0	0	0	0	1	0	0	0
Cyst of *Pentapharsodinium dalei*	58	77	47	39	65	43	32	42	51	29	28	24
Islandinium minutum	135	153	188	144	148	171	195	160	159	206	217	190
Islandinium ? cezare	0	9	10	3	3	10	1	9	2	9	4	4
Brigantedinium spp.	12	26	18	11	32	32	29	21	50	32	16	38
Selenopemphix quanta	18	14	7	8	5	5	2	2	0	1	1	0
Somme des dinokystes	**319**	**351**	**336**	**266**	**312**	**300**	**300**	**256**	**298**	**309**	**303**	**337**
Dinokystes/g	21211	45754	35377	21379	46241	43611	31676	38692	56716	35867	71624	26224
Dinokystes (cm^2/an)	2523	4659	3902	2746	4602	5466	4355	4405	6837	4486	11731	3070

Profondeur (cm)	**389**	**393**	**397**	**401**	**405**	**409**	**413**	**417**	**421**	**425**	**429**	**433**
Poids sec (g)	3,860	3,944	5,772	3,813	5,019	5,808	5,558	5,590	5,747	5,474	4,039	3,947
Volume (ml)	1,5	1,5	2,0	1,5	2,0	3,0	3,0	3,0	3,0	3,0	3,0	2,0
Nombre de *L. clavatum*/capsule	18583	18583	18583	18583	18583	18583	18583	18583	18583	18583	18583	18583
Lycopodium clavatum ajoutés	39	84	29	102	34	44	41	48	50	52	87	26
Nematosphaeropsis labyrinthus	1	4	0	1	0	1	1	0	0	0	0	0
Operculodinium centrocarpum	32	53	21	15	11	33	7	1	2	2	1	2
Spiniferites elongatus	12	23	11	9	5	14	1	1	0	4	0	2
Spiniferites ramosus	2	2	3	1	1	1	0	0	0	0	0	1
Spiniferites spp.	0	2	1	0	1	0	0	0	0	0	1	1
Cyst of *Pentapharsodinium dalei*	43	29	38	17	33	13	6	22	35	23	24	13
Islandinium minutum	157	198	170	252	235	237	252	245	244	231	244	262
Islandinium ? cezare	5	8	6	7	8	7	4	11	6	4	11	4
Brigantedinium spp.	40	19	50	24	18	30	36	28	28	43	29	45
Selenopemphix quanta	3	4	3	1	0	1	2	4	3	6	7	2
Somme des dinokystes	**295**	**342**	**303**	**327**	**312**	**337**	**309**	**312**	**318**	**313**	**317**	**332**
Dinokystes/g	36415	19185	33638	15626	33975	24505	25198	21607	20565	20435	16763	60116
Dinokystes (cm^2/an)	4685	2522	4854	1986	7674	4270	4202	3624	3546	3356	2031	10678

Profondeur (cm)	**441**	**445**	**449**	**453**	**457**	**461**	**465**	**469**	**473**	**477**	**481**	**485**
Poids sec (g)	4,305	4,013	3,905	3,943	3,796	4,252	4,393	5,867	6,063	4,461	4,388	3,981
Volume (ml)	2,0	2,0	2,0	2,0	2,0	2,0	2,0	2,5	3,0	2,0	2,0	2,0
Nombre de *L. clavatum*/capsule	18583	18583	18583	18583	18583	18583	18583	18583	18583	18583	18583	18583
Lycopodium clavatum ajoutés	78	151	131	95	154	25	65	43	25	42	53	82
Nematosphaeropsis labyrinthus	0	0	0	0	0	0	0	0	0	0	0	0
Operculodinium centrocarpum	2	1	0	1	1	0	0	0	3	1	1	1
Spiniferites elongatus	1	1	2	1	0	0	3	1	1	0	0	0
Spiniferites ramosus	0	1	1	0	0	0	0	0	0	0	0	0
Spiniferites spp.	0	0	0	0	1	0	0	0	0	0	0	0
Cyst of *Pentapharsodinium dalei*	11	4	12	14	23	9	9	11	20	16	20	5
Islandinium minutum	260	253	229	197	283	91	242	218	209	246	236	249
Islandinium ? cezare	4	3	4	4	4	1	2	3	6	3	5	6
Brigantedinium spp.	31	37	48	49	23	13	26	21	65	40	43	40
Selenopemphix quanta	1	4	1	1	3	0	0	4	1	1	0	0
Somme des dinokystes	**310**	**304**	**297**	**267**	**338**	**114**	**282**	**258**	**305**	**307**	**305**	**301**
Dinokystes/g	17157	9323	10790	13247	10809	19931	18351	19003	37391	30452	24373	17134
Dinokystes (cm^2/an)	3323	1684	1896	2350	1846	3813	3628	4014	6801	6112	4812	3070

Profondeur (cm)	**489**	**493**	**497**	**505**	**513**	**521**	**529**	**537**	**545**	**553**	**561**	**565**
Poids sec (g)	3,846	3,933	4,479	4,831	4,011	4,420	3,716	5,199	5,806	4,332	5,798	6,054
Volume (ml)	2,0	2,0	2,0	2,0	2,0	2,0	2,0	3,0	3,0	3,0	3,0	3,0
Nombre de *L. clavatum*/capsule	18583	18583	18583	18583	18583	18583	18583	18583	18583	18583	18583	18583
Lycopodium clavatum ajoutés	62	97	89	74	96	85	131	106	83	97	138	79
Nematosphaeropsis labyrinthus	0	0	1	0	0	0	0	0	0	0	0	0
Operculodinium centrocarpum	0	0	0	0	0	0	0	0	0	1	0	0
Spiniferites elongatus	1	0	0	0	0	0	0	0	0	0	0	0
Spiniferites ramosus	0	0	0	1	0	1	0	0	0	0	0	0
Spiniferites spp.	0	0	0	0	1	0	0	0	0	0	0	0
Cyst of *Pentapharsodinium dalei*	7	5	5	5	5	5	6	6	4	7	4	9
Islandinium minutum	247	233	273	276	254	252	246	247	246	238	260	226
Islandinium ? cezare	3	8	6	6	2	3	5	2	5	5	6	3
Brigantedinium spp.	51	56	44	41	39	49	50	45	57	58	43	72
Selenopemphix quanta	2		2	3	0	3	0	0	0	4	5	0
Somme des dinokystes	**311**	**302**	**331**	**332**	**301**	**313**	**307**	**300**	**312**	**313**	**318**	**310**
Dinokystes/g	24238	14709	15430	17259	14525	15480	11719	10116	12032	13843	7386	12044
Dinokystes (cm^2/an)	4195	2604	3110	3752	2622	3079	1960	1578	2096	1799	1285	2188

Profondeur (cm)	**577**	**585**	**593**	**601**	**625**	**673**	**709**	**805**	**901**	**1005**	**1101**
Poids sec (g)	5,037	5,988	5,714	5,873	6,017	6,022	6,344	6,538	4,910	3,272	2,983
Volume (ml)	3,0	3,0	3,0	3,0	3,0	3,0	3,0	3,0	2	2	2
Nombre de *L. clavatum*/capsule	18583	18583	18583	18583	18583	18583	18583	18584	18583	18583	18583
Lycopodium clavatum ajoutés	58	49	89	65	111	170	219	435	141	431	845
Nematosphaeropsis labyrinthus	0	0	0	0	0	0	0	0	0	0	0
Operculodinium centrocarpum	0	0	0	0	0	1	2	0	0	0	0
Spiniferites elongatus	0	0	0	0	0	0	0	0	0	0	0
Spiniferites ramosus	0	0	0	0	0	0	0	1	0	0	0
Spiniferites spp.	0	0	0	0	0	1	0	0	0	0	0
Cyst of *Pentapharsodinium dalei*	1	8	7	8	16	14	4	3	3	8	0
Islandinium minutum	261	277	239	257	240	233	241	251	124	216	148
Islandinium ? cezare	11	13	17	8	5	6	12	8	6	18	9
Brigantedinium spp.	57	20	36	37	39	52	56	48	38	58	165
Selenopemphix quanta	1	1	1	0	2	2	0	1	0	1	3
Somme des dinokystes	**331**	**319**	**300**	**310**	**302**	**309**	**315**	**312**	**171**	**301**	**325**
Dinokystes/g	21053	20203	10999	15089	8403	5609	4213	2039	4590	3967	2396
Dinokystes (cm^2/an)	3182	3629	1885	2659	1517	NA	NA	NA	NA	NA	NA

Tableau A.2 Dénombrements et concentrations des grains de pollen et autres palynomorphes dans la carotte MSM343300

	Profondeur (cm)	3	9	13	17	20	25	30	33	37	40	45	49
Pollens et autres palynomorphes	*Picea*	2	2	1	5	2	6	0	0	1	0	3	0,3
	Pinus	3	2	2	2	0	3	2	0	0	0,3	0	0
	Thuja	1	0	0	1	1	0	0	0	0	0	0	0
	Betula	0	0	1	1	0	0	1	1	2	0	0	0
	Alnus spp.	0	0	2	1	3	0	0	0	0	0	0	0
	Salix	0	0	0	0	0	0	0	0	0	0	0	0
	Ericaceae	1	0	0	0	0	1	0	0	0	0	0	0
	Somme des pollens	**7**	**4**	**6**	**10**	**6**	**10**	**3**	**1**	**3**	**0,3**	**3**	**0,3**
	Lycopodium spp.	0	0	1	0	0	0	0	0	1	0	0	0
	Spore monolète	0	1	1	2	3	1	0	0	1	0	0	0
	Spore trilète	2	0	1	2	0	0	2	0	2	0	0	1
	Oeufs de copépode	1	0	0	0	0	0	0	0	0	0	0	0
	Dinokystes remaniés	1	2	2	1	2	0	0	0	0	0	0	0
	Kyste P	0	0	0	0	0	0	0	0	0	0	0	0
	Réseaux organiques de foraminifère	**141**	**84**	**180**	**124**	**146**	**150**	**97**	**80**	**117**	**79**	**108**	**147**
	Halodinium	**59**	**51**	**101**	**62**	**66**	**93**	**56**	**46**	**67**	**59**	**78**	**63**
Concentrations	Pollens/g	502	565	858	1157	825	1000	288	116	514	53	470	34
	Halodinium/g	4231	7202	14447	7174	9071	9298	5367	5351	11475	10487	12223	7192
	Réseaux organiques de foraminifère/g	10110	43364	65590	51210	73331	47248	27314	30975	62123	36704	100354	101180
	Pollens (cm^2/an)	80	85	120	169	124	129	35	16	65	8	76	6
	Halodinium (cm^2/an)	673	1079	2012	1050	1359	1201	646	730	1459	1498	1981	1185
	Réseaux organiques de foraminifère (cm^2/an)	1609	1778	3585	2099	3006	1937	1120	1270	2547	2006	2743	2765

	Profondeur (cm)	52	57	61	65	69	73	77	81	85	89	93	97
Pollens et autres palynomorphes	*Picea*	3	0	1	1,3	1	2	2	0	0	0	0	2
	Pinus	0	0	0	0	0	1	0	0,3	2	2	1	0
	Thuja	0	0	0	0	0	0	0	0	0	0	0	0
	Betula	0	1	0	0	0	0	0	0	0	2	0	0
	Alnus spp.	0	0	0	0	0	0	0	0	0	0	0	0
	Salix	0	2	0	0	0	0	0	0	0	0	0	0
	Ericaceae	0	0	0	0	0	0	0	0	0	0	0	0
	Somme des pollens	**3**	**3**	**1**	**1,3**	**1**	**3**	**2**	**0,3**	**2**	**4**	**1**	**2**
	Lycopodium spp.	0	0	0	0	0	0	0	0	0	0	0	1
	Spore monolète	0	0	0	0	1	0	0	0	0	0	0	0
	Spore trilète	0	0	0	0	0	0	0	0	0	0	0	0
	Oeufs de copépode	0	0	0	0	0	0	0	0	0	0	0	0
	Dinokystes remaniés	0	0	0	0	0	0	0	0	1	1	0	0
	Kyste P	0	0	0	0	0	0	0	0	0	0	0	0
	Réseaux organiques de foraminifère	**130**	**123**	**127**	**99**	**111**	**95**	**84**	**79**	**78**	**117**	**94**	**81**
	Halodinium	**65**	**67**	**69**	**76**	**83**	**65**	**50**	**89**	**66**	**59**	**85**	**84**
Concentrations	Pollens/g	435	376	156	123	336	318	412	44	213	418	165	322
	Halodinium/g	9418	8395	10754	7165	27910	6883	10296	13065	7044	6164	14061	13527
	Réseaux organiques de foraminifère/g	58925	57146	78672	38332	128923	33953	62442	43182	25887	37489	64701	60214
	Pollens (cm^2/an)	56	57	25	21	48	44	61	7	27	53	28	61
	Halodinium (cm^2/an)	1208	1276	1752	1206	3952	952	1524	1994	898	775	2399	2560
	Réseaux organiques de foraminifère (cm^2/an)	2416	2343	3225	1571	5286	1392	2560	1770	1061	1537	2653	2469

	Profondeur (cm)	101	105	109	113	117	121	125	129	134	137	141	145
Pollens et autres palynomorphes	*Picea*	0,3	0	0	0	0	0	0,3	0	0	0	0	1
	Pinus	0,3	1	1	1	0	0	0	0	0	1,3	0	0
	Thuja	0	0	0	0	0	0	0	0	0	0	0	0
	Betula	0	0	0	0	0	0	0	0	3	0	0	2
	Alnus spp.	0	0	0	0	0	0	0	0	0	0	0	0
	Salix	0	0	0	0	0	0	0	0	0	0	0	0
	Ericaceae	0	0	0	0	0	0	0	0	0	0	0	0
	Somme des pollens	**0,6**	**1**	**1**	**1**	**0**	**0**	**0,3**	**0**	**3**	**1,3**	**0**	**3**
	Lycopodium spp.	1	0	0	0	0	0	2	0	0	0	0	0
	Spore monolète	0	0	0	1	0	0	0	0	0	0	0	0
	Spore trilète	0	0	0	0	0	0	0	0	0	0	0	0
	Oeufs de copépode	0	0	0	0	0	0	0	0	0	0	0	1
	Dinokystes remaniés	0	0	0	0	0	0	0	0	0	1	1	0
	Kyste P	0	0	0	0	0	0	0	0	0	0	0	0
	Réseaux organiques de foraminifère	**126**	**70**	**88**	**90**	**108**	**93**	**110**	**70**	**82**	**89**	**71**	**82**
	Halodinium	**59**	**44**	**80**	**33**	**64**	**53**	**46**	**57**	**60**	**60**	**71**	**94**
Concentrations	Pollens/g	81	354	153	251	0	0	56	0	1401	412	0	957
	Halodinium/g	7918	15584	12272	8275	21221	15467	8530	8516	28014	19030	31199	29990
	Réseaux organiques de foraminifère/g	80745	100066	51107	64329	133801	86414	56784	38263	101590	82697	87962	117220
	Pollens (cm^2/an)	16	59	24	29	0	0	13	0	203	66	0	176
	Halodinium (cm^2/an)	1550	2579	1905	967	3251	2019	1947	1277	4063	3048	3606	5509
	Réseaux organiques de foraminifère (cm^2/an)	3310	4103	2095	2637	5486	3543	4656	1569	5553	4521	3606	4806

	Profondeur (cm)	149	153	157	161	165	169	174	177	181	185	189	193
Pollens et autres palynomorphes	*Picea*	0	2	0	0	0	0	1	0	1	0	0	0
	Pinus	0	0	0	0	0	0	0	1	0	0	0	0
	Thuja	0	0	0	0	0	0	0	0	0	0	0	0
	Betula	0	0	0	0	0	0	0	0	0	0	1	1
	Alnus spp.	0	0	0	0	0	0	0	0	0	0	0	0
	Salix	0	0	0	0	0	0	0	0	0	0	0	0
	Ericaceae	0	0	0	0	0	0	0	0	0	0	0	0
	Somme des pollens	**0**	**2**	**0**	**0**	**0**	**0**	**1**	**1**	**1**	**0**	**1**	**1**
	Lycopodium spp.	0	0	0	0	0	0	0	0	0	0	1	0
	Spore monolète	1	0	0	0	0	0	1	0	0	0	0	1
	Spore trilète	0	0	0	1	0	0	0	0	0	0	0	0
	Oeufs de copépode	0	0	0	0	1	0	0	0	0	0	0	0
	Dinokystes remaniés	0	0	0	2	0	2	1	0	0	0	0	0
	Kyste P	0	0	0	0	0	0	0	0	0	1	0	0
	Réseaux organiques de foraminifère	**45**	**75**	**82**	**111**	**112**	**63**	**61**	**149**	**70**	**110**	**77**	**95**
	Halodinium	**19**	**42**	**31**	**44**	**66**	**38**	**11**	**103**	**45**	**101**	**37**	**50**
Concentrations	Pollens/g	0	604	0	0	0	0	207	116	116	0	163	118
	Halodinium/g	7318	12685	8064	8410	9642	9124	2277	11906	5199	15466	6043	5888
	Réseaux organiques de foraminifère/g	55752	60599	69267	71131	74337	53218	45346	56511	31731	60125	51107	37565
	Pollens (cm^2/an)	0	88	0	0	0	0	19	13	11	0	17	10
	Halodinium (cm^2/an)	1287	1855	1074	940	1095	802	204	1302	510	1380	614	494
	Réseaux organiques de foraminifère (cm^2/an)	3048	3313	2840	2371	1858	1330	1134	1884	793	1503	1278	939

	Profondeur (cm)	197	200	205	209	213	217	221	225	229	233	237	241
Pollens et autres palynomorphes	*Picea*	0	0	0	2	0	1	0	0	0	1	0	1
	Pinus	0	0	0	1	0	0	0	0	0	0	0	0
	Thuja	0	0	0	0	0	0	0	0	0	0	0	0
	Betula	0	0	0	0	1	0	0	0	0	0	0	0
	Alnus spp.	0	0	0	0	0	0	0	0	0	0	0	0
	Salix	0	0	0	0	0	0	0	0	0	0	0	0
	Ericaceae	0	0	0	0	0	0	0	0	0	0	0	0
	Somme des pollens	**0**	**0**	**0**	**3**	**1**	**1**	**0**	**0**	**0**	**1**	**0**	**1**
	Lycopodium spp.	0	1	0	0	0	0	0	1	1	2	0	0
	Spore monolète	0	0	0	0	0	0	0	0	0	0	0	0
	Spore trilète	0	0	0	0	0	0	0	0	0	0	0	0
	Oeufs de copépode	0	0	0	0	0	0	0	0	0	0	0	0
	Dinokystes remaniés	0	0	0	1	0	0	0	0	0	0	0	0
	Kyste P	0	0	0	0	0	0	0	0	0	0	0	0
	Réseaux organiques de foraminifère	**89**	**87**	**48**	**136**	**84**	**69**	**54**	**73**	**74**	**79**	**69**	**77**
	Halodinium	**51**	**63**	**41**	**46**	**54**	**65**	**33**	**66**	**44**	**38**	**45**	**42**
Concentrations	Pollens/g	0	0	0	309	193	210	0	0	0	299	0	143
	Halodinium/g	9989	26016	10083	4745	10438	13646	18261	12734	12800	11345	11208	6005
	Réseaux organiques de foraminifère/g	71912	134731	44603	56166	65045	55753	91229	58985	80894	81562	47493	40886
	Pollens (cm^2/an)	0	0	0	31	19	20	0	0	0	26	0	13
	Halodinium (cm^2/an)	1030	2439	952	475	1045	1313	1394	1333	1202	981	1032	557
	Réseaux organiques de foraminifère (cm^2/an)	1798	3368	1115	1404	1626	1394	2281	1475	2022	2039	1583	1022

	Profondeur (cm)	245	249	253	257	261	265	269	273	277	281	285	289
Pollens et autres palynomorphes	*Picea*	0	0	0	0	0	0	0	1	0	0	0	1
	Pinus	0	1	0	0	0	0	1	0	1	1	0	0
	Thuja	0	0	0	0	0	0	0	0	0	0	0	0
	Betula	0	0	0	0	0	0	0	0	0	0	1	0
	Alnus spp.	0	0	0	0	0	0	0	0	0	0	0	0
	Salix	0	0	0	0	0	0	0	0	0	0	0	0
	Ericaceae	0	0	0	0	0	0	0	0	0	0	0	0
	Somme des pollens	**0**	**1**	**0**	**0**	**0**	**0**	**1**	**1**	**1**	**1**	**1**	**1**
	Lycopodium spp.	0	1	1	1	0	0	0	2	0	0	2	0
	Spore monolète	0	0	0	0	0	0	1	0	0	0	1	0
	Spore trilète	0	1	2	0	0	0	0	0	0	0	0	0
	Oeufs de copépode	0	0	0	0	0	0	0	0	0	0	0	0
	Dinokystes remaniés	0	0	1	0	0	0	1	0	0	0	1	0
	Kyste P	0	0	0	0	0	0	0	0	0	0	0	0
	Réseaux organiques de foraminifère	**69**	**70**	**63**	**77**	**61**	**54**	**84**	**117**	**165**	**82**	**77**	**98**
	Halodinium	**45**	**51**	**38**	**52**	**58**	**36**	**26**	**45**	**36**	**48**	**32**	**49**
Concentrations	Pollens/g	0	245	0	0	0	0	125	170	188	182	225	164
	Halodinium/g	7329	12478	6203	8088	15824	5759	3249	7663	6761	8725	7185	8031
	Réseaux organiques de foraminifère/g	35621	56560	30022	44719	51529	32374	43364	51770	122652	46179	59624	65045
	Pollens (cm^2/an)	0	27	0	0	0	0	13	15	19	19	26	17
	Halodinium (cm^2/an)	774	1374	604	755	1225	540	336	664	669	901	826	813
	Réseaux organiques de foraminifère (cm^2/an)	1187	1885	1001	1118	1288	809	1084	1726	3066	1539	1987	1626

	Profondeur (cm)	293	297	301	305	309	313	317	321	325	329	333	337
Pollens et autres palynomorphes	*Picea*	1	0	0	0	0	0	0	0	1	2	1	0
	Pinus	0	1	0	0	0	0	0	0	0	0	0	0
	Thuja	0	0	0	0	0	0	0	0	0	0	0	0
	Betula	0	1	1	1	1	0	0	0	0	0	0	1
	Alnus spp.	0	0	0	0	0	0	0	0	0	0	0	0
	Salix	0	0	0	0	0	0	0	0	0	0	0	0
	Ericaceae	0	0	0	0	0	0	0	0	0	0	0	0
	Somme des pollens	**1**	**2**	**1**	**1**	**1**	**0**	**0**	**0**	**1**	**2**	**1**	**1**
	Lycopodium spp.	0	0	0	2	0	0	0	0	0	0	0	0
	Spore monolète	0	0	0	0	2	0	0	0	0	0	0	0
	Spore trilète	0	0	0	0	0	0	0	0	0	1	0	0
	Oeufs de copépode	0	0	0	0	0	0	0	0	0	0	0	0
	Dinokystes remaniés	0	0	0	0	0	3	0	2	0	0	0	0
	Kyste P	0	0	0	0	0	1	0	0	0	0	0	0
	Réseaux organiques de foraminifère	**57**	**85**	**76**	**87**	**73**	**74**	**55**	**109**	**81**	**107**	**51**	**176**
	Halodinium	**41**	**33**	**21**	**34**	**24**	**33**	**21**	**48**	**28**	**21**	**17**	**88**
Concentrations	Pollens/g	288	527	173	222	224	0	0	0	240	175	211	278
	Halodinium/g	11806	8695	3643	7543	5382	4611	3559	6696	6720	1838	3581	24449
	Réseaux organiques de foraminifère/g	70620	87757	56497	76991	71402	40449	39314	63303	94081	40584	59239	233620
	Pollens (cm^2/an)	31	52	19	22	24	0	0	0	29	19	29	33
	Halodinium (cm^2/an)	1270	852	390	752	587	451	375	697	813	199	494	2920
	Réseaux organiques de foraminifère (cm^2/an)	1765	2194	1412	1925	1785	1011	983	1582	2352	1014	1481	5840

	Profondeur (cm)	341	345	349	353	357	361	365	369	373	377	381	385
Pollens et autres palynomorphes	*Picea*	0	0	1	0	0	0	0	0	0	0	1	0
	Pinus	0	0	0	0	0	0	0	0	0	0	0	0
	Thuja	0	0	0	0	0	0	0	0	0	0	0	0
	Betula	0	0	0	0	0	0	0	0	0	1	0	0
	Alnus spp.	0	0	0	0	0	0	0	0	0	0	0	0
	Salix	0	0	0	0	0	0	0	0	0	0	0	0
	Ericaceae	0	0	0	0	0	0	0	0	0	0	0	0
	Somme des pollens	**0**	**0**	**1**	**0**	**0**	**0**	**0**	**0**	**0**	**1**	**1**	**0**
	Lycopodium spp.	0	0	1	0	0	1	0	0	0	0	0	0
	Spore monolète	0	0	0	0	0	0	0	0	0	0	0	0
	Spore trilète	0	0	0	0	0	0	0	0	0	1	0	1
	Oeufs de copépode	0	0	0	0	0	0	0	0	0	0	0	0
	Dinokystes remaniés	0	0	0	0	0	0	0	0	1	0	0	0
	Kyste P	0	0	0	0	2	0	0	0	1	0	0	0
	Réseaux organiques de foraminifère	**96**	**96**	**77**	**80**	**116**	**108**	**111**	**113**	**107**	**100**	**108**	**99**
	Halodinium	**35**	**70**	**31**	**48**	**32**	**57**	**45**	**39**	**43**	**67**	**46**	**55**
Concentrations	Pollens/g	0	0	105	0	0	0	0	0	0	116	236	0
	Halodinium/g	2327	9125	3264	3858	4743	8286	4751	5895	8184	7777	10874	4280
	Réseaux organiques de foraminifère/g	37963	50975	44721	33042	102655	59032	64465	58333	73647	58077	125440	36078
	Pollens (cm^2/an)	0	0	12	0	0	0	0	0	0	15	39	0
	Halodinium (cm^2/an)	277	929	360	496	472	1038	653	671	987	973	1781	501
	Réseaux organiques de foraminifère (cm^2/an)	759	1274	894	826	1711	1968	1611	1944	2455	1452	4181	902

	Profondeur (cm)	389	393	397	401	405	409	413	417	421	425	429	433
Pollens et autres palynomorphes	*Picea*	0	0	0	0	0	0	0	0	0	0	0	0
	Pinus	0	0	0	0	0	0	0	0	0	0	0	0
	Thuja	0	0	0	0	0	0	0	0	0	0	0	0
	Betula	0	0	0	1	0	0	0	0	0	1	1	0
	Alnus spp.	0	0	0	0	0	0	0	0	0	0	0	0
	Salix	0	0	0	0	0	0	0	0	0	0	0	0
	Ericaceae	0	0	0	0	0	0	0	0	0	0	0	0
	Somme des pollens	**0**	**0**	**0**	**1**	**0**	**0**	**0**	**0**	**0**	**1**	**1**	**0**
	Lycopodium spp.	0	1	0	0	0	0	0	1	0	1	0	0
	Spore monolète	0	0	0	0	0	0	0	0	0	0	0	0
	Spore trilète	0	1	0	1	0	1	0	3	0	0	0	0
	Oeufs de copépode	0	0	0	0	0	0	0	0	0	0	0	0
	Dinokystes remaniés	0	0	0	0	0	0	0	1	0	0	0	0
	Kyste P	1	0	0	0	0	0	0	0	0	0	0	0
	Réseaux organiques de foraminifère	**89**	**89**	**78**	**106**	**76**	**127**	**78**	**89**	**100**	**107**	**65**	**73**
	Halodinium	**50**	**57**	**36**	**73**	**41**	**94**	**57**	**65**	**81**	**76**	**51**	**77**
Concentrations	Pollens/g	0	0	0	48	0	0	0	0	0	65	53	0
	Halodinium/g	6172	3198	3997	3488	4465	6835	4648	4502	5238	4962	2697	13943
	Réseaux organiques de foraminifère/g	42411	19693	49988	19316	41543	53643	35359	34462	37172	38244	13888	52179
	Pollens (cm^2/an)	0	0	0	6	0	0	0	0	0	11	6	0
	Halodinium (cm^2/an)	794	420	577	443	1008	1191	775	755	903	815	327	2477
	Réseaux organiques de foraminifère (cm^2/an)	1414	656	1250	644	1869	1609	1061	1034	1115	1147	417	2348

	Profondeur (cm)	441	445	449	453	457	461	465	469	473	477	481	485
Pollens et autres palynomorphes	*Picea*	0	1	0	0	0	0	0	0	0	0	0	0
	Pinus	0	0	0	0	1	0	0	0	0	0	0	0
	Thuja	0	0	0	0	0	0	0	0	0	0	0	0
	Betula	0	1	2	0	0	0	0	0	0	1	0	0
	Alnus spp.	0	0	0	0	0	0	0	0	0	0	0	0
	Salix	0	0	0	0	0	0	0	0	0	0	0	0
	Ericaceae	0	0	0	0	0	0	0	0	0	0	0	0
	Somme des pollens	**0**	**2**	**2**	**0**	**1**	**0**	**0**	**0**	**0**	**1**	**0**	**0**
	Lycopodium spp.	0	0	0	0	0	0	0	0	0	0	0	0
	Spore monolète	0	0	0	0	0	1	0	0	0	0	0	0
	Spore trilète	0	1	0	1	1	0	0	0	0	0	0	1
	Oeufs de copépode	0	0	0	0	0	0	0	0	0	0	0	0
	Dinokystes remaniés	0	0	0	0	0	0	0	0	0	0	0	0
	Kyste P	0	0	0	0	0	0	0	0	0	0	0	1
	Réseaux organiques de foraminifère	**50**	**65**	**78**	**106**	**69**	**27**	**72**	**92**	**48**	**98**	**57**	**87**
	Halodinium	**33**	**39**	**62**	**71**	**59**	**31**	**89**	**73**	**25**	**63**	**44**	**69**
Concentrations	Pollens/g	0	61	73	0	32	0	0	0	0	99	0	0
	Halodinium/g	1826	1196	2252	3523	1876	5420	5792	5377	3065	6249	3516	3928
	Réseaux organiques de foraminifère/g	11916	8003	11069	20739	8330	20074	20589	39765	35685	43365	19990	19720
	Pollens (cm^2/an)	0	11	13	0	5	0	0	0	0	20	0	0
	Halodinium (cm^2/an)	354	216	396	625	320	1037	1145	1136	557	1254	694	704
	Réseaux organiques de foraminifère (cm^2/an)	536	360	498	933	375	903	926	1431	1070	1951	899	887

	Profondeur (cm)	489	493	497	505	513	521	529	537	545	553	561	565
Pollens et autres palynomorphes	*Picea*	0	0	0	0	2	0	0	0	0	0	0	0
	Pinus	0	1	0	0	0	0	0	0	0	0	0	0
	Thuja	0	0	0	0	0	0	0	0	0	0	0	0
	Betula	0	0	0	0	0	0	0	0	0	0	0	0
	Alnus spp.	0	0	0	0	0	0	0	0	0	0	0	0
	Salix	0	0	0	0	0	0	0	0	0	0	0	0
	Ericaceae	0	0	0	0	0	0	0	0	0	0	0	0
	Somme des pollens	**0**	**1**	**0**	**0**	**2**	**0**	**0**	**0**	**0**	**0**	**0**	**0**
	Lycopodium spp.	0	0	0	0	0	0	0	1	1	1	0	0
	Spore monolète	0	0	0	0	0	0	0	0	0	0	0	0
	Spore trilète	0	0	0	0	0	0	0	0	1	0	0	0
	Oeufs de copépode	0	0	0	0	0	0	0	0	0	0	0	0
	Dinokystes remaniés	0	0	0	0	0	0	0	0	0	0	0	0
	Kyste P	1	0	1	0	0	0	0	0	0	0	0	0
	Réseaux organiques de foraminifère	**82**	**104**	**86**	**101**	**83**	**84**	**113**	**68**	**78**	**92**	**118**	**96**
	Halodinium	**74**	**65**	**94**	**96**	**64**	**74**	**73**	**111**	**83**	**96**	**106**	**77**
Concentrations	Pollens/g	0	49	0	0	97	0	0	0	0	0	0	0
	Halodinium/g	5767	3166	4382	4991	3088	3660	2787	3743	3201	4246	2462	2992
	Réseaux organiques de foraminifère/g	24581	19928	17961	25368	16071	18369	16033	11926	17469	17629	15896	22588
	Pollens (cm^2/an)	0	9	0	0	17	0	0	0	0	0	0	0
	Halodinium (cm^2/an)	998	560	883	1085	557	728	466	584	557	552	428	543
	Réseaux organiques de foraminifère (cm^2/an)	1106	897	808	1141	723	826	721	358	524	529	477	677

	Profondeur (cm)	577	585	593	601	625	673	709	805	901	1005	1101
Pollens et autres palynomorphes	*Picea*	0	0	1	0	0	0	0	1	0	0	0
	Pinus	0	0	0	0	0	1	0	1	0	1	2
	Thuja	0	0	0	0	0	0	0	0	0	0	0
	Betula	0	0	0	0	0	0	5	1	0	0	0
	Alnus spp.	0	0	0	0	0	0	0	0	0	0	0
	Salix	0	0	0	0	0	0	0	0	0	0	0
	Ericaceae	0	0	0	0	0	0	0	0	0	0	0
	Somme des pollens	**0**	**0**	**1**	**0**	**0**	**1**	**5**	**3**	**0**	**1**	**2**
	Lycopodium spp.	0	0	0	1	0	1	2	0	0	0	0
	Spore monolète	0	0	0	0	0	0	0	0	0	0	0
	Spore trilète	0	0	0	0	0	1	3	1	0	0	0
	Oeufs de copépode	0	0	0	0	0	0	0	0	0	0	0
	Dinokystes remaniés	0	0	1	0	0	0	0	0	0	0	0
	Kyste P	0	0	0	0	0	0	0	0	0	0	1
	Réseaux organiques de foraminifère	**65**	**75**	**76**	**46**	**63**	**95**	**73**	**155**	**31**	**53**	**25**
	Halodinium	**57**	**66**	**49**	**52**	**45**	**35**	**19**	**38**	**4**	**18**	**12**
Concentrations	Pollens/g	0	0	37	0	0	18	67	20	0	13	15
	Halodinium/g	3625	4180	1791	2531	1252	635	254	248	107	237	88
	Réseaux organiques de foraminifère/g	20831	28449	15874	13157	10553	10391	6201	6628	4091	2288	553
	Pollens (cm^2/an)	0	0	6	0	0	NA	NA	NA	NA	NA	NA
	Halodinium (cm^2/an)	548	751	307	446	226	NA	NA	NA	NA	NA	NA
	Réseaux organiques de foraminifère (cm^2/an)	625	853	476	395	316	NA	NA	NA	NA	NA	NA

Tableau A.3 Reconstitution des conditions de surface à partir des abondances relatives des dinokystes de la carotte MSM343300 en utilisant la méthode des analogues modernes (Base de données du Geotop; n=1492)

Profondeur (cm)	Température de surface d'été (°C)	Salinité de surface d'été (psu)	Nombre de mois de glace de mer	Productivité ($gC\ m^{-2}/an$)
3	10,93	28,50	3,24	382,63
9	9,32	30,46	3,69	252,76
13	10,99	30,57	3,36	260,89
17	10,04	30,39	3,40	293,28
20	10,62	30,13	3,35	309,03
25	9,83	30,48	3,64	252,51
30	8,29	30,48	3,87	226,75
33	4,30	32,43	5,17	152,43
37	9,76	30,14	3,73	243,82
40	6,09	31,99	4,17	177,65
45	15,33	28,84	3,21	388,31
49	9,96	30,55	3,61	241,68
52	9,63	30,97	1,80	266,50
57	6,29	31,72	4,61	170,53
61	7,66	30,87	4,04	205,24
65	5,76	31,24	6,72	180,22
69	2,80	31,26	8,08	110,67
73	2,94	32,73	7,33	109,76
77	8,34	30,01	5,64	199,29
81	8,08	32,11	1,64	240,31
85	12,15	28,99	4,06	334,08
89	7,79	30,16	6,18	198,46
93	6,32	30,70	6,37	194,11
97	9,64	31,20	1,76	284,49
101	12,37	30,41	3,25	290,86
105	11,77	30,37	2,51	326,03
109	12,54	30,28	2,46	328,17
113	9,66	30,51	3,19	263,39
117	11,94	29,18	4,12	343,63
121	10,09	29,75	4,63	273,57
125	11,23	30,49	3,33	265,60
129	10,01	30,18	3,36	244,23
134	12,01	29,76	3,19	366,93
137	14,12	28,82	3,42	378,63
141	7,23	30,12	5,79	222,49
145	9,94	30,32	3,49	235,79
149	14,46	28,78	3,58	391,53
153	12,86	28,95	3,84	347,55

Reconstitution des conditions de surface à partir des abondances relatives des dinokystes de la carotte MSM343300 en utilisant la méthode des analogues modernes (Base de données du Geotop; n=1492) (suite)

Profondeur (cm)	Température de surface d'été (°C)	Salinité de surface d'été (psu)	Nombre de mois de glace de mer	Productivité (gC m^{-2}/an)
157	9,57	29,52	5,00	286,03
165	12,01	29,07	3,93	336,94
169	9,74	30,55	3,13	263,66
173	12,28	28,91	4,19	330,97
177	10,02	29,76	3,43	299,13
181	8,35	30,50	2,17	328,54
185	8,37	30,16	5,23	252,49
189	14,51	28,77	3,58	392,22
193	9,54	30,96	1,83	286,14
197	11,20	29,29	3,72	341,04
200	10,30	29,31	4,37	295,59
205	13,26	29,39	2,82	359,79
209	11,09	30,53	2,41	324,00
213	9,21	29,65	5,24	240,16
217	8,93	30,29	2,32	336,64
221	12,52	29,53	2,83	357,34
225	7,53	30,09	5,63	232,81
229	9,62	29,87	5,04	262,78
233	7,07	30,14	5,52	298,48
237	10,58	30,82	2,74	334,14
241	11,37	30,62	2,78	338,05
245	5,88	32,14	4,13	225,50
249	5,88	28,26	6,83	248,18
253	6,02	31,67	3,80	208,92
257	11,76	28,89	3,18	398,76
261	10,34	29,37	4,47	281,82
265	5,99	30,58	6,48	215,08
269	8,98	30,94	2,08	292,00
273	11,55	28,88	3,20	412,17
277	10,32	29,72	2,84	384,96
281	9,14	30,23	3,40	280,67
285	9,40	31,00	3,20	278,77
289	11,57	28,89	3,20	411,18
293	9,68	30,76	2,21	290,77
297	10,21	29,29	2,78	379,52
301	11,33	28,90	3,83	364,57
305	11,44	28,83	3,21	416,88
309	12,61	29,72	3,13	362,59
313	11,59	28,90	3,20	410,36
317	10,28	29,94	2,73	363,93

Reconstitution des conditions de surface à partir des abondances relatives des dinokystes de la carotte MSM343300 en utilisant la méthode des analogues modernes (Base de données du Geotop; n=1492) (suite)

Profondeur (cm)	Température de surface d'été (°C)	Salinité de surface d'été (psu)	Nombre de mois de glace de mer	Productivité ($gC\ m^{-2}/an$)
321	11,19	31,06	2,31	326,67
325	11,35	28,79	3,21	420,57
329	11,04	30,79	2,67	328,52
333	10,15	29,94	2,76	375,65
337	10,17	30,64	2,63	325,01
341	9,41	29,25	3,89	385,47
345	6,08	32,33	3,67	216,17
349	10,07	29,60	4,80	269,13
353	8,27	31,25	4,17	211,37
357	4,35	30,84	7,53	182,21
361	3,84	28,97	7,67	198,69
365	6,03	31,72	5,38	181,29
369	3,46	28,96	8,06	193,88
373	6,24	31,91	4,53	156,11
377	2,62	31,31	8,12	126,77
381	6,06	31,80	5,54	153,11
385	2,83	29,32	8,70	120,14
389	6,13	30,35	6,38	188,73
393	7,72	31,99	2,62	219,69
397	8,11	30,35	4,52	227,25
401	2,67	32,42	7,41	103,59
405	4,17	31,78	6,46	132,05
409	3,00	32,16	7,41	102,48
413	1,29	31,68	8,51	99,36
417	1,75	31,98	7,89	112,72
421	1,57	31,95	7,83	119,67
425	5,12	31,14	6,59	196,54
429	3,82	31,24	6,98	167,28
433	1,82	32,01	7,76	108,95
441	1,68	31,98	7,80	116,05
445	1,84	32,11	7,94	115,03
449	1,41	31,43	8,27	110,77
453	1,76	32,00	7,86	112,42
457	1,68	31,99	7,75	114,11
461	1,42	31,46	8,03	112,89
465	1,24	31,37	8,16	115,78
469	1,60	31,66	8,04	110,61
473	1,57	31,60	8,21	101,07
477	1,58	31,97	7,80	120,12

Reconstitution des conditions de surface à partir des abondances relatives des dinokystes de la carotte MSM343300 en utilisant la méthode des analogues modernes (Base de données du Geotop; n=1492) (suite)

Profondeur (cm)	Température de surface d'été (°C)	Salinité de surface d'été (psu)	Nombre de mois de glace de mer	Productivité (gC m^{-2}/an)
481	1,58	31,96	7,83	119,79
485	1,51	31,64	7,97	117,36
489	1,45	31,48	8,27	110,32
497	0,66	31,29	9,42	91,31
505	1,35	31,48	8,63	110,43
513	1,45	31,29	8,21	110,35
521	1,61	31,61	8,17	110,53
529	1,12	31,17	8,60	112,39
537	1,44	31,27	8,22	110,16
545	1,09	31,13	8,63	111,96
553	1,74	32,13	7,82	118,32
561	1,42	31,56	8,59	110,05
565	1,35	31,35	8,05	112,42
577	1,24	31,42	8,72	110,65
585	0,68	31,20	9,16	106,38
593	0,68	31,22	9,02	105,62
601	1,14	31,20	8,61	112,67
625	1,56	31,58	8,06	110,55
673	1,58	31,96	7,83	120,16
709	1,41	31,86	8,34	116,80
805	1,27	31,36	8,68	110,35
909	0,71	30,93	9,08	104,23
1013	0,82	31,17	9,17	102,76
1109	1,99	32,27	8,32	105,51

Figure A.1 Abondances relatives des dinokystes et concentrations des principaux palynomorphes

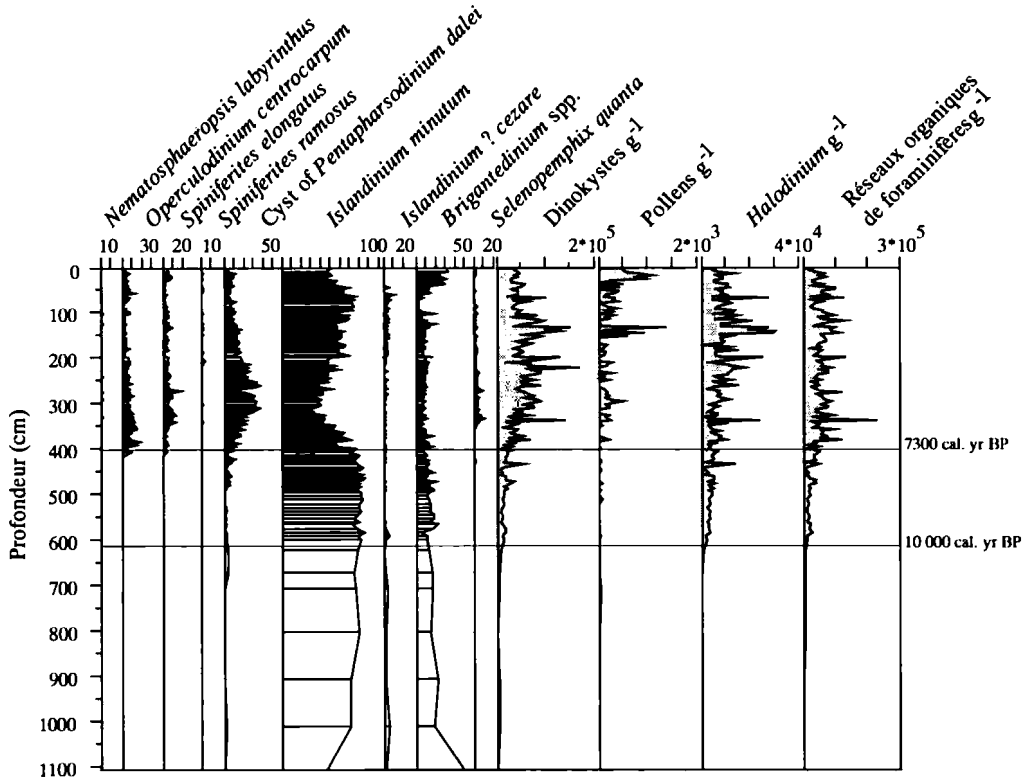

Figure A.2 Reconstitutions de surface de la température, salinité, couvert de glace et productivité de la carotte MSM343300 en utilisant la méthode des analogues modernes (Base de données du Geotop n=1492)

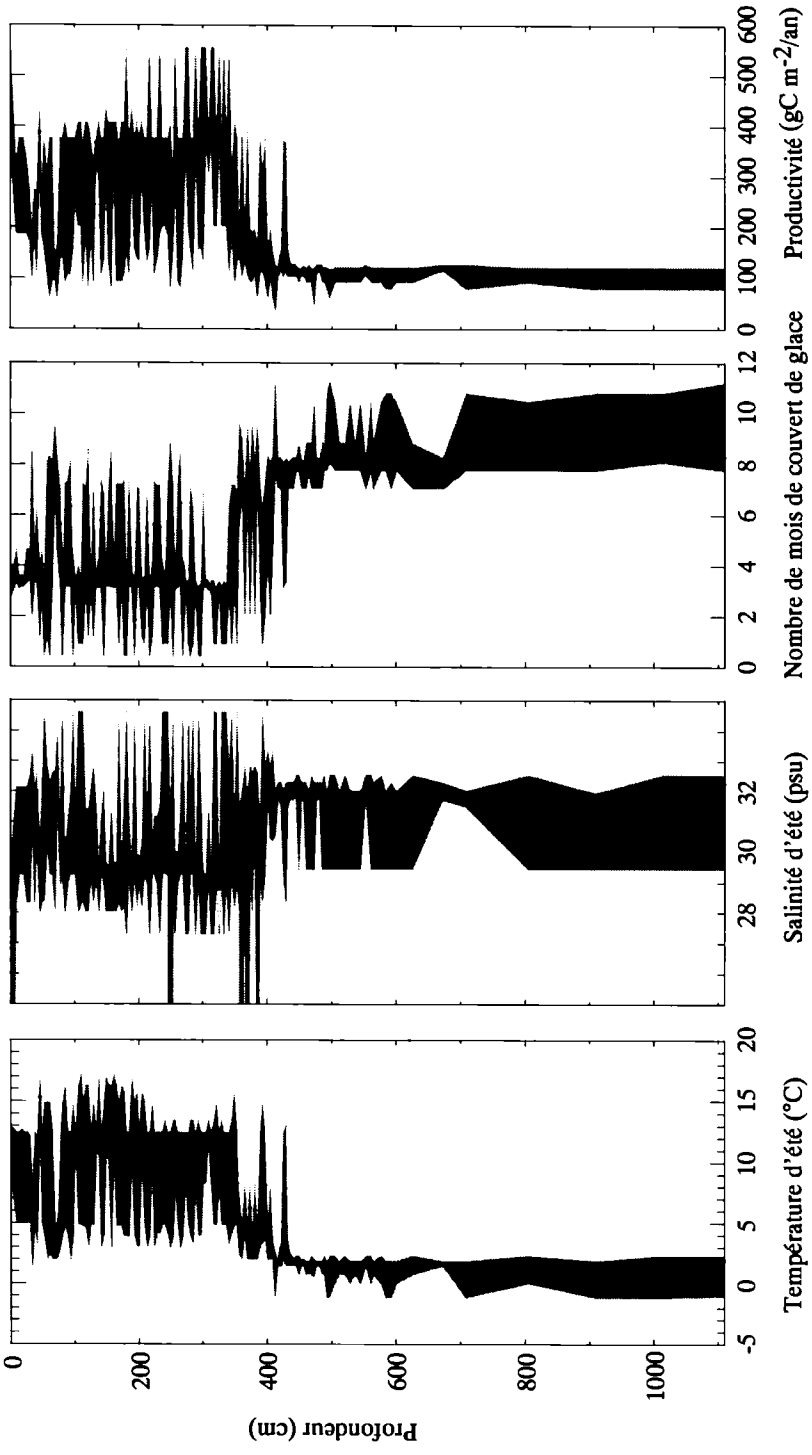

Les valeurs reconstituées sont représentés par les points et ligne noirs, un lissage des données (3 valeurs) est représenté par la ligne grise foncée et les marges d'erreur sont représentées en gris.

Figure A.3 Analyse en composantes principales réalisée à partir des abondances relatives des dinokystes de la carotte MSM343300

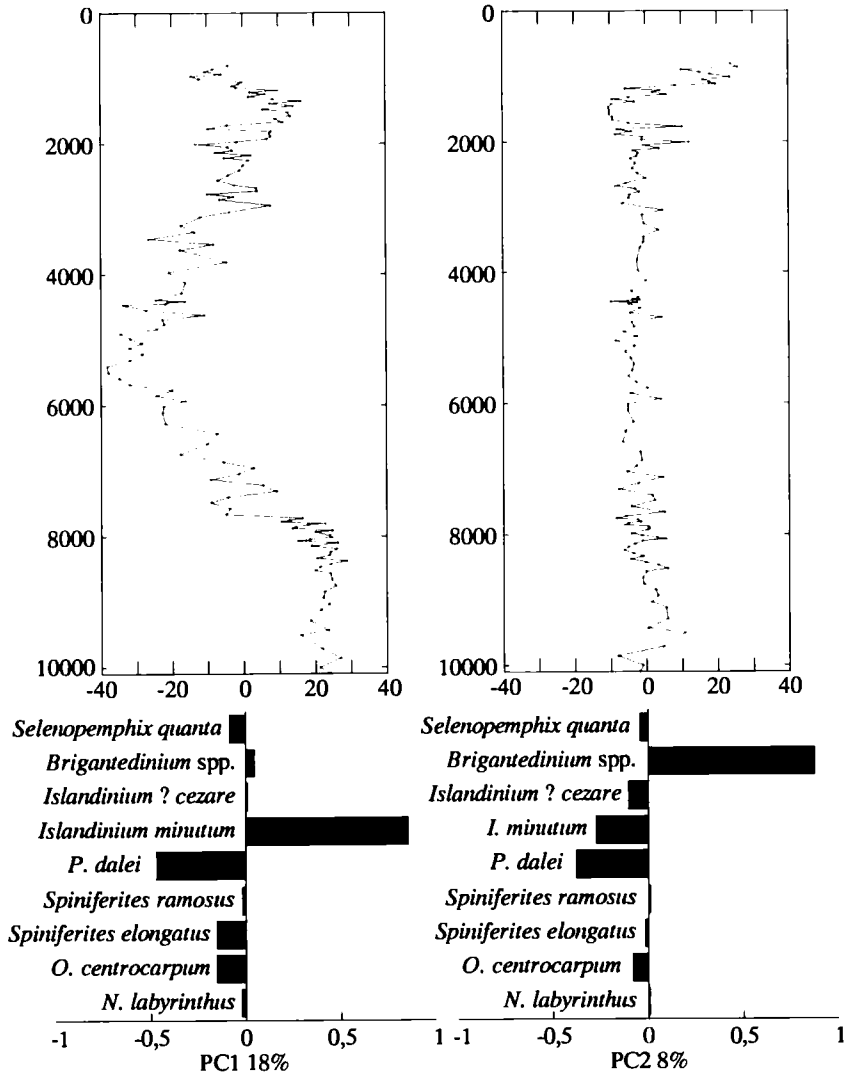

APPENDICE B

RESULTATS DES ANALYSES ISOTOPIQUES

Tableau B.1 : Résultats des analyses isotopiques ($\delta^{13}C$) effectuées sur la matière organique dans la carotte MSM343300

Tableau B.2 : Résultats des analyses isotopiques ($\delta^{13}C$ et $\delta^{18}O$) des tests carbonatés du foraminifère benthique *Islandiella norcrossi* dans la carotte MSM343300

Tableau B.3 : Résultats des analyses isotopiques ($\delta^{13}C$ et $\delta^{18}O$) des tests carbonatés du foraminifère benthique *Nonionellina labradorica* dans la carotte MSM343300

Figure B.1 : Compositions isotopiques ($\delta^{13}C$) de la matière organique dans la carotte MSM343300

Figure B.2 : Compositions isotopiques des foraminifères benthiques *Islandiella norcrossi* (losanges) et *Nonionellina labradorica* (cercles) dans la carotte MSM343300

Tableau B.1 Résultats des analyses isotopiques ($\delta^{13}C$) effectuées sur la matière organique dans la carotte MSM343300

$\delta^{13}C$ MO exprimé en ‰ vs VPDB (±0,1‰ à 1σ)

Profondeur (cm)	$\delta^{13}C$	Profondeur (cm)	$\delta^{13}C$	Profondeur (cm)	$\delta^{13}C$
61	-21,61	369	-22,16	561	-22,83
69	-22,85	377	-22,96	561	-23,05
81	-23,26	385	-25,46	569	-22,58
85	-21,92	393	-22,35	577	-22,94
93	-21,51	397	-23,69	577	-22,83
101	-21,84	401	-24,02	589	-22,64
105	-21,10	409	-24,36	597	-22,98
117	-21,74	413	-23,73	597	-22,99
129	-21,30	413	-24,50	617	-23,32
149	-21,67	417	-23,65	633	-23,08
153	-21,43	425	-23,06	633	-22,92
161	-21,32	425	-23,81	657	-23,21
173	-21,57	433	-23,79	685	-24,11
173	-21,69	441	-24,58	701	-23,08
197	-22,16	445	-23,77	717	-23,33
201	-21,66	449	-24,62	741	-24,50
209	-21,73	453	-26,98	765	-24,49
221	-22,63	457	-23,49	781	-24,02
229	-21,61	457	-24,23	821	-24,28
245	-22,63	461	-22,62	845	-24,70
249	-22,10	469	-22,88	861	-23,78
249	-23,11	469	-22,78	877	-23,47
257	-22,39	477	-22,73	877	-23,35
265	-21,81	477	-22,53	893	-23,65
273	-22,54	485	-22,86	909	-23,92
281	-21,71	485	-23,22	909	-23,54
289	-23,01	493	-22,77	925	-23,84
298	-22,12	501	-22,56	941	-23,94
301	-22,30	501	-22,69	941	-23,63
317	-22,06	509	-22,64	957	-23,98
325	-22,22	517	-22,85	973	-24,14
333	-22,30	517	-22,60	973	-23,62
333	-21,96	525	-22,97	990	-23,49
341	-22,32	533	-22,69		
349	-22,23	545	-23,15		
349	-22,02	545	-22,86		
361	-22,05	553	-22,58		

Tableau B.2 Résultats des analyses isotopiques ($\delta^{13}C$ et $\delta^{18}O$) des tests carbonatés du foraminifère benthique *Islandiella norcrossi* dans la carotte MSM343300

Fraction 150-250 µm			Fraction >250 µm		
Profondeur (cm)	**$\delta^{13}C$**	**$\delta^{18}O$**	**Profondeur (cm)**	**$\delta^{13}C$**	**$\delta^{18}O$**
20	-0,36	3,24	73	0,03	3,32
25	-0,08	3,39	153	-0,19	3,21
30	-0,69	3,26	185	-0,64	3,20
40	-0,27	3,32	197	-0,33	3,21
45	-0,20	3,29	311	-0,23	3,27
49	-0,35	3,41	549	-0,33	3,92
52	-0,11	3,39			
61	-0,29	3,31			
65	-0,29	3,56			
77	-0,24	3,23			
81	-0,35	3,32			
89	-0,32	3,30			
93	-0,25	3,31			
97	-0,37	3,48			
101	-0,46	3,36			
105	-0,34	3,35			
109	-0,35	3,31			
113	-0,34	3,33			
117	-0,33	3,40			
121	-0,32	3,27			
125	-0,42	2,86			
149	-0,54	3,29			
157	-0,40	3,35			
161	-0,39	3,39			
165	-0,47	3,24			
169	-0,42	3,13			
173	-0,38	3,22			
177	-0,39	3,20			
181	-0,30	3,17			
186	-0,43	3,10			
189	-0,53	3,23			
193	-0,42	3,36			
197	-0,54	3,11			
200	-0,41	3,27			
205	-0,24	3,38			
209	-0,46	3,11			
213	-0,33	3,22			
217	-0,35	3,13			

Résultats des analyses isotopiques ($\delta^{13}C$ et $\delta^{18}O$) des tests carbonatés du foraminifère benthique *Islandiella norcrossi* dans la carotte MSM343300 (suite)

Fraction 150-250 µm

Profondeur (cm)	$\delta^{13}C$	$\delta^{18}O$
221	-0,39	3,32
225	-0,24	3,25
229	-0,29	3,26
233	-0,34	3,28
237	-0,29	3,29
241	-0,28	3,27
245	-0,50	3,16
249	-0,28	3,19
253	-0,19	2,28
257	-0,25	3,28
265	-0,33	3,26
269	-0,19	3,22
281	-0,37	3,15
285	-0,55	3,28
289	-0,23	3,35
293	-0,41	3,29
297	-0,42	3,11
301	-0,32	3,39
305	-0,25	3,39
309	-0,28	3,28
313	-0,21	3,43
321	-0,12	3,34
325	-0,30	3,31
329	-0,34	3,44
333	-0,62	2,58
337	-0,16	3,39
341	-0,20	3,38
393	-0,53	3,49
409	-1,60	1,47
469	-4,72	3,38
549	-0,53	4,00
567	-0,54	3,97
837	-0,72	3,98
969	-1,91	3,76

Tableau B.3 Résultats des analyses isotopiques ($\delta^{13}C$ et $\delta^{18}O$) des tests carbonatés du foraminifère benthique *Nonionellina labradorica* dans la carotte MSM343300

Fraction 150-250 µm			Fraction >250 µm		
Profondeur (cm)	**$\delta^{13}C$**	**$\delta^{18}O$**	**Profondeur (cm)**	**$\delta^{13}C$**	**$\delta^{18}O$**
93	-1,17	2,39	47	-1,00	3,56
179	-1,15	3,02	77	-0,82	3,57
187	-1,39	3,07	81	-0,95	3,40
197	-1,74	2,77	85	-1,74	3,08
207	-1,82	3,40	89	-1,16	3,34
293	-1,64	3,12	93	-0,74	3,46
299	-1,99	3,35	97	-1,22	3,55
329	-1,60	3,54	103	-1,56	3,43
337	-1,91	3,44	111	-1,99	3,35
409	-1,74	3,43	177	-1,55	3,24
469	-6,30	2,16	181	-1,74	3,52
			185	-1,61	3,15
			189	-1,63	3,40
			193	-1,52	3,53
			197	-1,84	3,25
			205	-1,87	3,29
			209	-1,71	3,00
			213	-1,18	3,21
			221	-1,55	3,29
			233	-1,54	3,36
			293	-2,36	3,24
			297	-2,53	3,30
			301	-2,29	3,46
			305	-2,66	3,45
			309	-2,93	3,07
			333	-2,41	3,35
			337	-1,80	3,35
			409	-2,04	3,69
			469	-6,41	3,37
			469	-6,03	3,58

Figure B.1 **Compositions isotopiques ($\delta^{13}C$) de la matière organique dans la carotte MSM343300**

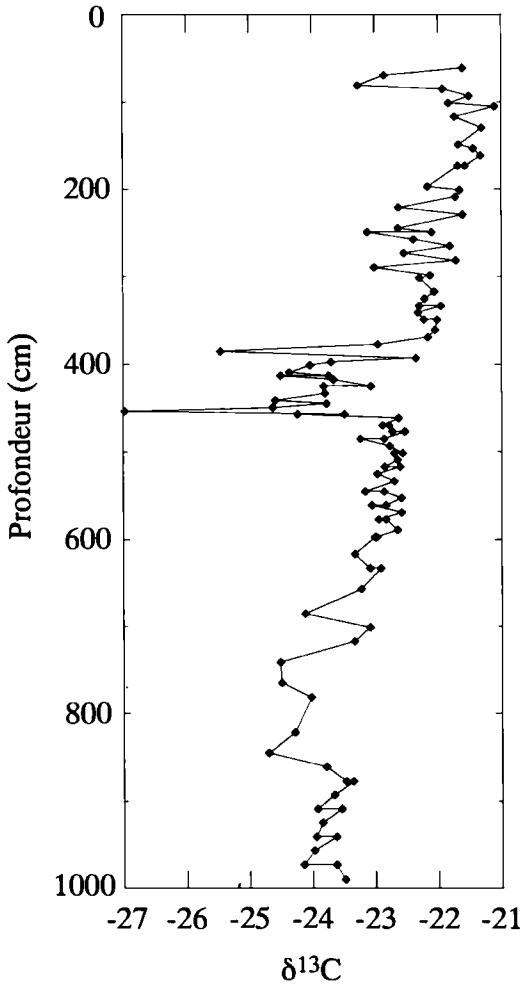

Figure B.2 Compositions isotopiques des foraminifères benthiques *Islandiella norcrossi* (losanges) et *Nonionellina labradorica* (cercles) dans la carotte MSM343300

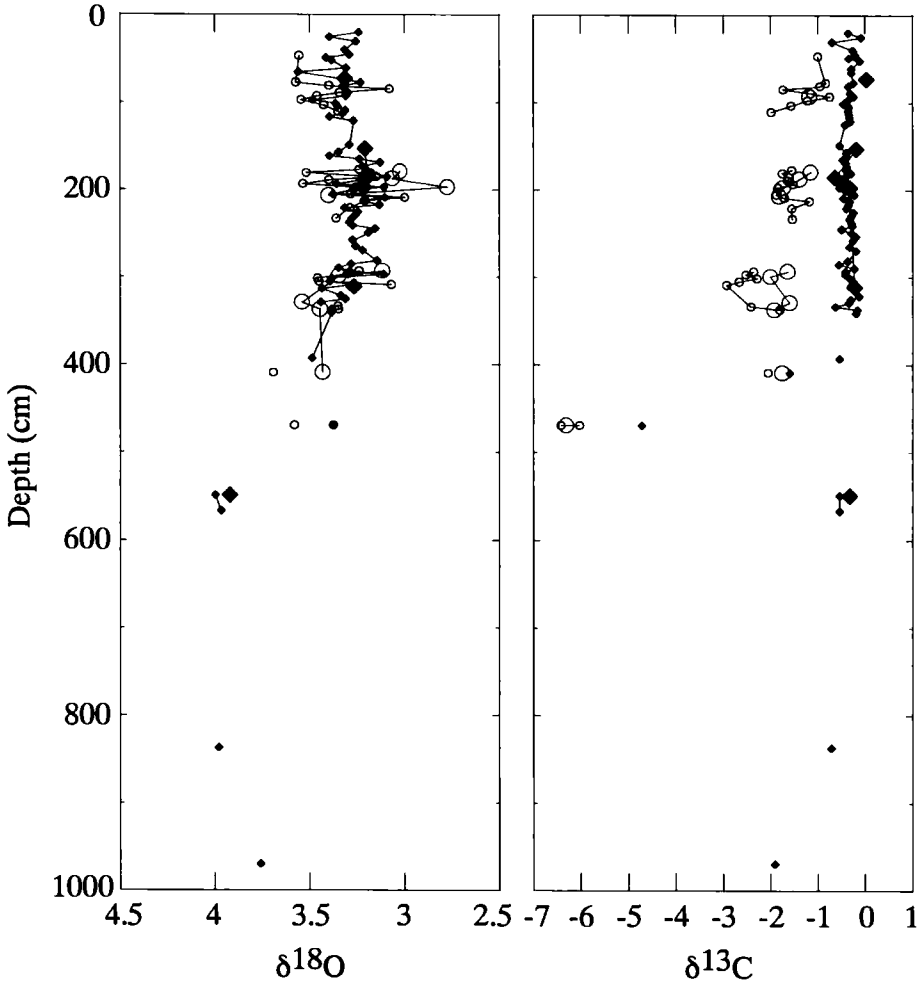

Les foraminifères de plus grande taille (>250 μm) et de plus petite taille (150-250 μm) ont été analysés.

APPENDICE C

APPENDICE DINFLUENCE DES KYSTES D'*ISLANDINIUM*? *CEZARE* DANS LES RECONSTITUTIONS DE SURFACE DE FAIBLES DIVERSITÉS TAXONOMIQUES

Les valeurs des reconstitutions climatiques sont obtenues à partir des fonctions de transfert. Celles-ci sont réalisées à partir de la base de données du Geotop de 1492 analogues modernes. Les échantillons à 429, 457, 473 et 481 cm (~8200 à ~7000 ans BP) ont retenu notre attention. À ces niveaux, aucun *I.* ? *cezare* n'a été compté et les reconstitutions montraient une diminution drastique de la salinité. Où la diversité taxonomique est faible, la présence ou l'absence d'un taxon peut donc avoir une importante significative, notamment puisque les dénombrements sont exprimés en pour mille et qu'une transformation logarithmique est appliquée. Ces échantillons ont été comptés une seconde fois et la présence de *I.* ? *cezare* a été notée. Cette fois, la reconstitution réalisée ne montre aucune variation majeure de la salinité.

Ces différentes reconstitutions permettent de mettre à l'avant que la reconstitution de la salinité pose plusieurs difficultés en raison des différences importantes de salinité en Arctique notamment en raison des décharges d'eaux de fonte qui contribuent à une importante diminution de la salinité. En contrepartie, les reconstitutions des températures de surface demeurent inchangées venant appuyer la solidité de la reconstitution de température et l'indépendance existant entre la température et la salinité que permettent les reconstitutions à l'aide des kystes de dinoflagellés.

En somme, si l'identification d'un taxon pose problème, il serait mieux de le grouper par espèce. Comme on peut le constater à partir de la reconstitution effectuée

à partir du regroupement *Islandinium minutum* et *Islandinium*? *cezare*, il n'y a pas de diminution marquée de la salinité.

Figure D.1 Comparaison des reconstitutions climatiques à partir de la technique des analogues modernes

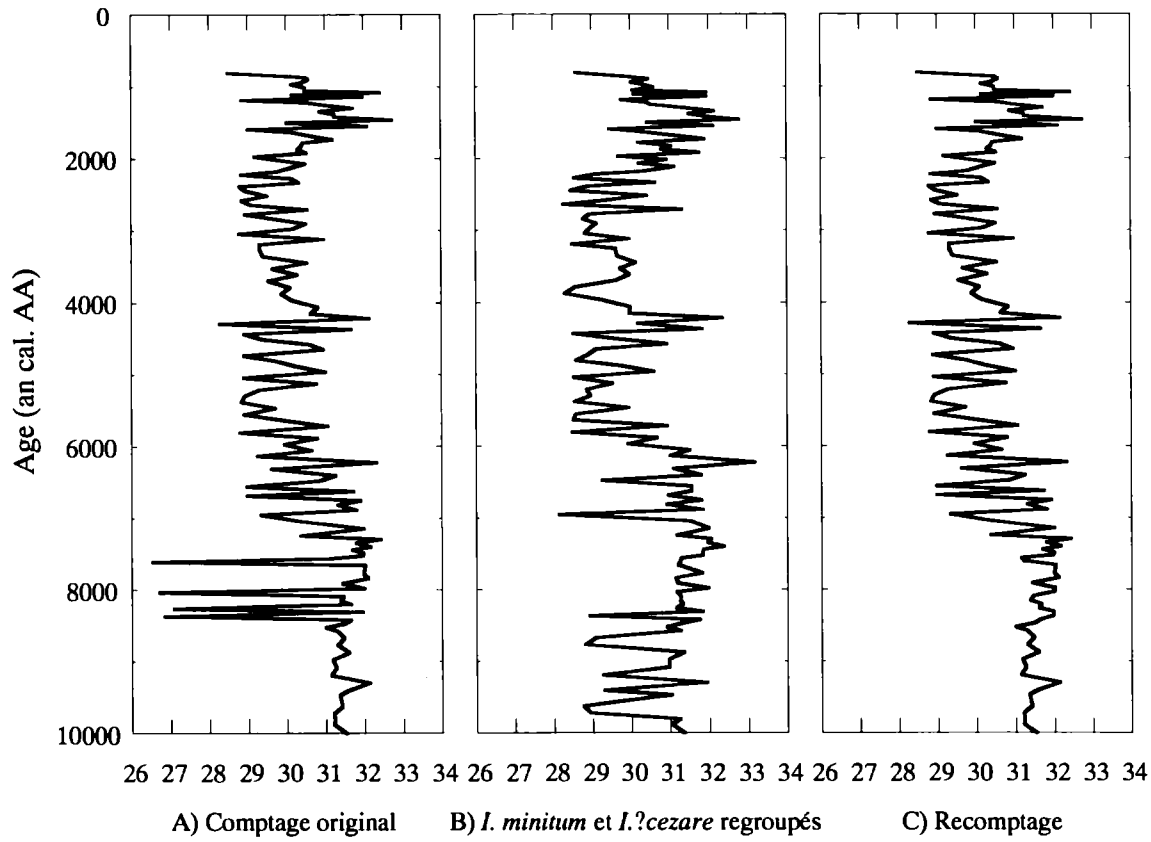

A) Aucun *I.* ? *cezare* n'a été compté aux niveaux 429, 457, 473 et 481 cm. B) Regroupement des taxons *I. minutum* et *I.* ? *cezare* (comptage original). C) Recomptage des niveaux 429, 457, 473 et 481 cm.

APPENDICE D

PLANCHE PHOTOGRAPHIQUE

Planche D.1 Photographies des dinokystes et palynomorphes de la carotte MSM343300 réalisées au microscope optique

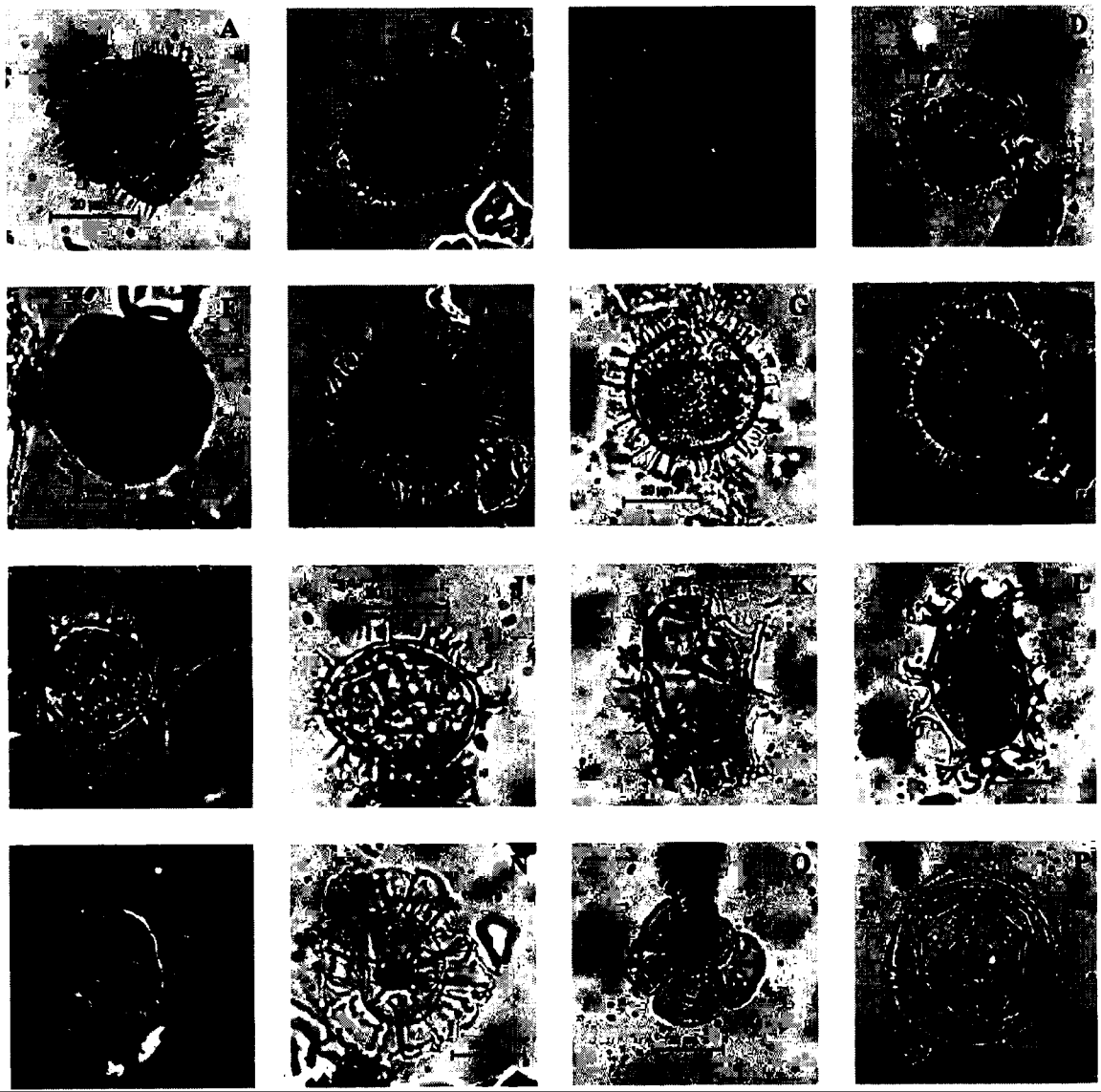

Légende de la planche photographique

A-B-C : *Islandinium minutum* (Harland and Reid in Harland *et al.*, 1980)

D : *Islandinium* ? *cezare* (de Vernal *et al.*, 1989 ex de Vernal *in* Rochon *et al.*, 1999)

E : *Bringantedinium* spp. Reid, 1977 ex Lentin and Williams, 1993

F : *Selenopemphix quanta* (Bradford, 1975) Matsuoka, 1985

G-H : *Operculodinium centrocarpum* sensu Wall and Dale, 1966

I-J : Cyst of *Pentapharsodinium dalei* Indelicato & Loeblich III, 1986

K-L : *Spiniferites elongatus* Reid, 1974

M : *Spiniferites ramosus* (Ehrenberg, 1838) Mantell, 1854 sensu lato

N : *Nematosphaeropsis labyrinthus* (Ostenfeld, 1903) Reid, 1974

O : Réseau organique de foraminifère

P : *Halodinium* spp.

BIBLIOGRAPHIE GÉNÉRALE

Berger, André. 1988. «Milankovitch theory and climate». *Reviews of Geophysics*, vol. 26, no 4, p. 624-657.

Bond, G., B. Kromer, J. Beer, R. Muscheler, M. N. Evans, W. Showers, S. Hoffmann, R. Lotti-Bond, I. Hajdas et G. Bonani. 2001. «Persistent solar influence on North Atlantic climate during the Holocene». *Science*, vol. 294, no 5549, p. 2130-2136. En ligne. <http://www.ncbi.nlm.nih.gov/pubmed/11739949>.

Buch, Erik. 1982. «Review of oceanographic conditions in Sub area 0 and 1 during the 1970–79 decade». *NAFO Sci. Coun. Studies*, vol. 5, p. 43-50.

Holland, David M., Robert H. Thomas, Brad de Young, Mads H. Ribergaard et Bjarne Lyberth. 2008. «Acceleration of Jakobshavn Isbræ triggered by warm subsurface ocean waters». *Nature Geoscience*, vol. 1, no 10, p. 659-664.

IPCC. 2012. «Managing the Risks of Extreme Events and Disasters to Advance Climate Change Adaptation. A Special Report of Working Groups I and II of the Intergovernmental Panel on Climate Change». C.B. Field, V. Barros, T.F. Stocker, D. Qin, D.J. Dokken, K.L. Ebi, M.D. Mastrandrea, K.J. Mach, G.-K. Plattner, S.K. Allen, M. Tignor, P.M. Midgley. Cambridge, UK and New York, NY, USA, Cambridge University Press: 582 pp.

IPCC. 2013. «Climate Change 2013: The Physical Science Basis. Contribution of Working Group I to the Fifth Assessment Report of the Intergovernmental Panel on Climate Change» [Stocker, T.F., D. Qin, G.-K. Plattner, M. Tignor, S.K. Allen, J. Boschung, A. Nauels, Y. Xia, V. Bex and P.M. Midgley (eds.)]. Cambridge University Press: 1535 pp.

Joughin, Ian, W. Abdalati et M. Fahnestock. 2004. «Large fluctuations in speed on Greenland's Jakobshavn Isbrae glacier». *Nature*, vol. 432, p. 608-610.

McCarthy, David. 2011. «Late Quaternary ice-ocean interactions in central West Greenland». Durham University.

NODC (National Oceanographic Data Center). 2001. «World Ocean Database 2001, Scientific Data Sets, Observed and Standard Level Oceanographic». *Data. National Oceanic and Atmospheric Administration*, Boulder, Colorado.

Perner, K., M. Moros, A. Jennings, J. Lloyd et K. Knudsen. 2013. «Holocene palaeoceanographic evolution off West Greenland». *The Holocene*, vol. 23, no 3, p. 374-387.

Perner, K., M. Moros, J. M. Lloyd, A. Kuijpers, R. J. Telford et J. Harff. 2011. «Centennial scale benthic foraminiferal record of late Holocene oceanographic variability in Disko Bugt, West Greenland». *Quaternary Science Reviews*, vol. 30, no 19-20, p. 2815-2826.

Ren, Jian, Hui Jiang, Marit-Solveig Seidenkrantz et Antoon Kuijpers. 2009. «A diatom-based reconstruction of Early Holocene hydrographic and climatic change in a southwest Greenland fjord». *Marine Micropaleontology*, vol. 70, no 3-4, p. 166-176.

Rignot, E., et P. Kanagaratnam. 2006. «Changes in the velocity structure of the Greenland Ice Sheet». *Science*, vol. 311, no 5763, p. 986-990. En ligne. <http://www.scopus.com/inward/record.url?eid=2-s2.0-33144459778&partnerID=40&md5=b7b91223f63465f03b9a3a9c5908ddd2>.

Roberts, David H., et Antony J. Long. 2005. «Streamlined bedrock terrain and fast ice flow, Jakobshavns Isbrae, West Greenland: implications for ice stream and ice sheet dynamics». *Boreas*, vol. 34, no 1, p. 25-42.

Seidenkrantz, Marit-Solveig, Hanne Ebbesen, Steffen Aagaard-Sørensen, Matthias Moros, Jeremy M. Lloyd, Jesper Olsen, Mads Faurschou Knudsen et Antoon Kuijpers. 2013. «Early Holocene large-scale meltwater discharge from Greenland documented by foraminifera and sediment parameters». *Palaeogeography, Palaeoclimatology, Palaeoecology*, vol. 391, p. 71-81.

Tang, Charles C. L., Charles K. Ross, Tom Yao, Brian Petrie, Brendan M. DeTracey et Ewa Dunlap. 2004. «The circulation, water masses and sea-ice of Baffin Bay». *Progress in Oceanography*, vol. 63, no 4, p. 183-228.

Weidick, A., et O. Bennike. 2007. «Quaternary glaciation history and glaciology of Jakobshavn Isbræ and the Disko Bugt region, West Greenland: A review». p. 1-78. En ligne. <http://www.scopus.com/inward/record.url?eid=2-s2.0-39549086991&partnerID=40&md5=d1079db37d9767e70e2b6d71ba345841.